Journal of Elasticity **59:** 319–355, 2000.

Finite Scale Microstructures in Nonlocal Elasticity

XIAOFENG REN[1,⋆] and LEV TRUSKINOVSKY[2,⋆⋆]
[1]*Department of Mathematics and Statistics, Utah State University, Logan, UT 84322, U.S.A. E-mail: ren@sunfs.math.usa.edu*
[2]*Department of Aerospace Engineering and Mechanics, University of Minnesota, Minneapolis, MN 55455, U.S.A. E-mail: trusk@aem.umn.edn*

Received 22 March 1999; in revised form 21 January 2000

Dedicated to Roger Fosdick.

Abstract. In this paper we develop a simple one-dimensional model accounting for the formation and growth of globally stable finite scale microstructures. We extend Ericksen's model [9] of an elastic "bar" with nonconvex energy by including both oscillation-inhibiting and oscillation-forcing terms in the energy functional. The surface energy is modeled by a conventional strain gradient term. The main new ingredient in the model is a nonlocal term which is quadratic in strains and has a negative definite kernel. This term can be interpreted as an energy associated with the long-range elastic interaction of the system with the constraining loading device. We propose a scaling of the problem allowing one to represent the global minimizer as a collection of localized interfaces with explicitly known long-range interaction. In this limit the augmented Ericksen's problem can be analyzed completely and the equilibrium spacing of the periodic microstructure can be expressed as a function of the prescribed average displacement. We then study the inertial dynamics of the system and demonstrate how the nucleation and growth of the microstructures result in the predicted stable pattern. Our results are particularly relevant for the modeling of twined martensite inside the austenitic matrix.

1. Introduction

Self-accommodating coherent mixtures of solid phases are observed in shape memory alloys and other "active" materials in a variety of stable equilibrium configurations. Typically these microstructures exhibit almost periodic patterns of piecewise homogeneous elastic domains. Some of the most important properties of "active" materials are due to the fact that the microstructures are mobile so that large reversible deformation can be accomplished by the motion of the domain boundaries.

Intensive research in recent years has led to well defined constitutive theories which explained some general features of the equilibrium microstructures. It is now well established that it is the non(quasi)-convexity of the elastic energy which is

⋆ Supported in part by NSF grant DMS-9703727.
⋆⋆ Supported in part by NSF grants DMS-9501433, DMS-9803572.

responsible for the formation of elastic domains. The adaptation of the thermoelasticity theory was successful in predicting the orientation of the microstructures and in quantifying the overall response of the phase mixtures (see the reviews of Roytburd [28], Khachaturian [17], Luskin [20], Müller [23], Ball and James [1], Pitteri and Zanzotto [25]). The classical nonlinear elasticity, however, was unable to predict the finite scale of the equilibrium domains, neither was it sufficient to describe such important dynamic phenomena as the microstructure nucleation and growth. A considerable challenge is still presented by a self-consistent description of the complex structure of the martensite-austenite interfaces separating the twinned regions from the homogeneous phases.

It has long been clear that an adequate theory should contain at least one intrinsic length scale. Recent attempts to bring a length scale into the theory were focused on gradient models which represent high order singular perturbation of the classical elasticity and are capable of describing "thick" phase boundaries (e.g., Kohn and Müller [19]). The most complete understanding was achieved in a one-dimensional setting where the analysis can be carried out explicitly. Unfortunately, the one-dimensional gradient models, having the merit of simplicity, fail to describe some significantly non-one-dimensional effects, in particular the strain compatibility constraint and, what is more important for the subject of this paper, the constraint provided by the fixation of the boundary displacements. This last limitation precludes the refinement of the microstructure in principle (e.g., Carr et al. [6]). The problem does not disappear if the gradient term describing the short range interaction is substituted by a fully nonlocal term with a positive definite kernel (e.g., Fosdick and Mason [12–14], Brandon et al. [5], Rogers and Truskinovsky [27], Bates et al. [4], Ren and Winter [26]).

The fact that the observed microstructures (at least away from the boundaries) are grossly one-dimensional suggests that the one-dimensional framework may still be sufficient for modeling the main features of the domain layering. To obtain a description of the stable finite scale microstructures in terms of a one-dimensional ansatz, it is necessary to include both oscillation-inhibiting and oscillation-forcing terms in the governing equations. The corresponding models must not only penalize sharp interfaces but also account for the incompatibility of the fixed displacements on the boundary with the coarse spacing of elastic domains. The two competing interactions operate at drastically different length scales: atomic distances in the case of surface effects and the size of the sample in the case of the boundary constraint. In order to preserve the long range component of the interaction in the one-dimensional setting one needs to introduce an additional non-constitutive compensating term into the energy functional; formally this term has the appearance of a nonlocal coupling. The most well known example of such a quasi-one-dimensional ansatz is the Pierls's model in the theory of dislocations [24].

Sometimes, as in the case of a shape-memory epitaxial thin film on an elastic substratum, the one-dimensional model is applicable directly. In this case, the

elastic foundation plays the role of an oscillation-forcing agent (Ball et al. [2]). The "effective" one-dimensional setting was adopted in a series of recent papers (Müller [23], Truskinovsky and Zanzotto [33, 34], Vainchten et al. [35]), where the Ericksen's bar model with nonconvex energy was augmented by the introduction of the strain gradient surface energy and where the displacements of the bar were coupled quadratically with a rigid substratum. The "foundation" term, which depends on displacements (rather than strains), can also be rewritten in terms of strains as a nonlocal term with a nonpositive definite interaction kernel. The model was shown to present a rich variety of stable and metastable finite scale microstructures; it is quite clear that the refinement tendency is due to the negative definite ("antiferromagnetic") component of the kernel.

In this paper we adopt the idea of a negative definite kernel as a general framework in which the nonlocal oscillation-forcing interactions can be modeled in a one-dimensional setting. Exactly like in the Peierls's model, one can understand the corresponding contributions to the energy as a result of minimizing out the "non-one-dimensional" components of the elastic fields and expressing the energy of the body in terms of the relevant "order parameters" only. The reason why the nonlocal terms are quadratic can be traced to the fact that the elastic problem can usually be considered linear with respect to all variables other than "order parameters". Explicit examples of the equilibrium relaxation of the "irrelevant" components of the strain field leading to the nonpositive definite contribution to the nonlocal interaction kernel, can be found in [16, 18].

Although the power law kernel would be more appropriate, for technical reasons we focus in what follows on a model with a (negative definite) *exponential* kernel. The same model with a positive definite exponential kernel was previously considered by Rogers and Truskinovsky [27] who showed that the equivalent local problem reduces to the classical Timoshenko model in the theory of elastic beams (see also [5, 7, 12–14]). Here we perform an analogous reduction to the local model and obtain a static FitzHugh–Nagumo theory [11] which is known to describe stable periodic patterns. We study in some detail a particular asymptotic limit of the theory presuming a physically natural separation of scales: in our approximation the thickness of the phase boundaries (controlled by the strain gradient term in the energy) is much smaller than the range of nonlocal interaction. As a result one can neglect the nonlocal term inside the transition layers and drop the gradient term in the description of the interaction between the phase boundaries. We perform a rigorous Γ-limit analysis leading to the discrete problem describing N interacting phase boundaries. In the one-dimensional setting the phase boundaries are represented by point "particles"; the resulting effective "interatomic potential" can be calculated explicitly. We then show that the distribution of interfaces is necessarily periodic and compute equilibrium spacing of the corresponding lattice.

An obvious drawback of our analytic approach is the focus on the absolute minimizer only. It is a serious limitation, since the previous experience with analogous models (e.g., [33, 34]) strongly suggests a rich variety of local minimizers

(metastable states). To check the accessibility of the calculated microstructures we study dynamics. Our dynamical model, which includes both inertia and viscosity, describes spontaneous nucleation and propagation of the microstructures; the pattern apparently settles down to a time independent state. As we show, the limiting microstructure is periodic and the period is in close agreement with the one calculated for the global minimizer. Effectively, our numerical results present a first example of self-consistent simulation of the kinetics of austenite–martensite interface.

The remaining sections of the paper are organized as follows. In Section 2 we revisit the Ericksen's bar model on an elastic foundation and provide a motivation for the introduction of a nonlocal energy with negative kernel. In Section 3 we specify the exponential kernel and prove the equivalence of our nonlocal theory to the local FitzHugh–Nagumo model in the theory of excitable reaction–diffusion systems. In Section 4 we nondimensionalize the governing equations and suggest a scaling leading to the desired separation of scales. The Γ-limit and the reduction to a finite-dimensional problem are performed in Section 5; the technical results are collected in the Appendix. In Section 6 we show that in the equilibrium configuration the effective "interface-particles" form a periodic pattern and calculate explicitly the energy of the corresponding lattice. In Section 7 we find, among all admissible lattices, the one which corresponds to the absolute minimum of the energy and give a simple approximate formula for the number of interfaces per unit length. In Section 8 we formulate our dynamical model. Computational results describing nucleation, propagation and stabilization of the microstructures are presented in Section 9. In Section 10 we briefly discuss an extension of the model capable of simulating sharp (rather than diffuse) phase transition fronts. In the last section we summarize the results and formulate the unsolved problems.

2. The Motivation

We begin with the problem studied by Ericksen [9]. Consider an elastic bar with nonconvex energy density. The bar is placed in a hard loading device which means that the total displacement is fixed. The mathematical problem reduces to constrained minimization of the energy functional

$$F(w) = \int_0^L W(w)\,\mathrm{d}x. \tag{2.1}$$

Here $w(x) = Du(x)$ is the strain field, $u(x)$ is the displacement field and D is the operator of differentiation in x. Without loss of generality, we may assume that the energy density $W(w)$ is a non-negative double-well function with zeros at -1 and $+1$; for example, $W(w) = (w^2 - 1)^2$ (see Figure 1). Physically, the wells correspond to different crystallographic phases of the material or different symmetry-related variants of the same phase (twins). The double-well energy function gives rise to a characteristic nonmonotone stress–strain relation $\sigma(w) = W(w)$

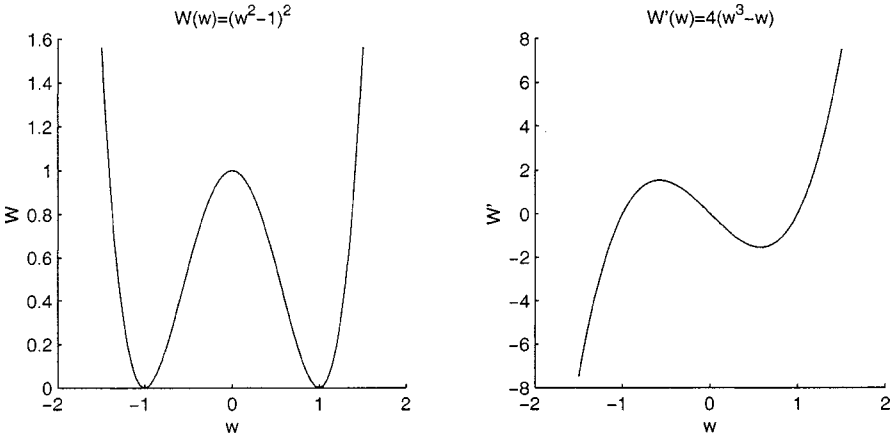

Figure 1. A double well energy $W(w)$ and its derivative $W'(w)$.

(see Figure 1). The constraint on the total displacement (or average strain) can be formulated in the form

$$\int_0^L w\,\mathrm{d}x = d. \tag{2.2}$$

Suppose that the trivial (homogeneous) solution of the variational problem (2.1), (2.2) is unstable, which takes place, for example, at $d = 0$ (see [9]). The double-well structure of the energy clearly favors configurations where the displacement gradient takes values at the bottoms of the wells, and the energy minimizing configuration represents a mixture of homogeneous states (phases) with w equal $+1$ or -1. The phase distribution must be compatible with the condition (2.2) specifying the corresponding "volume" fractions. This one-dimensional constraint is too weak, however, to affect the fineness of the microstructure which remains unspecified in this classical setting.

To penalize sharp interfaces between the phases one can include a surface energy into the model, by introducing a strain gradient term into the energy functional

$$F(w) = \int_0^L \big[W(w) + a|Dw|^2\big]\mathrm{d}x. \tag{2.3}$$

Here $a > 0$ is a constant parameter representing an internal length scale; throughout this paper we denote by D, $D^2, \ldots$ the corresponding derivatives of a function with respect to the space variable.

The strain gradient penalization turns sharp interfaces into diffuse ones and produces minimizers with one interface at most [6]. To obtain a fine scale microstructure with many interfaces, one needs to include an additional interaction into the system which acts against the strain gradient coarsening. For example, one can place the bar on an elastic foundation and consider the following functional [34]:

$$F(w) = \int_0^L \big[W(w) + a|Dw|^2 + bu^2\big]\mathrm{d}x. \tag{2.4}$$

Here $b > 0$ is a constant parameter which brings another length scale into the model. The "foundation" term is of non-constitutive nature which is clear from its dependence on displacements rather than displacement gradients. The introduction of this term guarantees the refinement of the microstructure: the strain gradients can now stay near the bottoms of the wells only if the displacements $u(x)$ are small and that requires fine oscillations of the displacement gradient. A competition between the coarsening tendency due to the surface energy and the refinement tendency due to the foundation term stabilizes the finite scale microstructures. In the limit $a \to 0$, $b \to 0$ the number of interfaces is finite and depends on the limit of the non-dimensional combination $c = ab^{-2}$ [34].

We observe that the " foundation" term in (2.4) can be rewritten in terms of strain gradients as well. Assume for determinacy that $u(0) = -d/2$ and $u(L) = d/2$ and let $\xi_x(y)$ be the characteristic function of the set $(0, x)$. Then

$$\begin{aligned}\int_0^L u^2\,\mathrm{d}x &= \int_0^L \left[\int_0^L \xi_x(y)w(y)\,\mathrm{d}y - \frac{d}{2}\right]^2 \mathrm{d}x \\ &= \int_0^L \left[\int_0^L \left(\xi_x(y)w(y) - \frac{1}{2}w(y)\right)\mathrm{d}y\right]^2 \mathrm{d}x \\ &= \int_0^L \int_0^L w(x)w(y)\left\{\int_0^L \left[\xi_z(x) - \frac{1}{2}\right]\left[\xi_z(y) - \frac{1}{2}\right]\mathrm{d}z\right\}\mathrm{d}x\,\mathrm{d}y.\end{aligned}$$

Now, since

$$\int_0^L \left[\xi_z(x) - \frac{1}{2}\right]\left[\xi_z(y) - \frac{1}{2}\right]\mathrm{d}z = \frac{L}{4} - \max\{x, y\} + \frac{1}{2}(x + y),$$

we obtain

$$F(w) = \int_0^L \big[W(w) + a|Dw|^2\big]\mathrm{d}x + b\int_0^L \int_0^L K(x, y)w(x)w(y)\,\mathrm{d}x\,\mathrm{d}y, \qquad (2.5)$$

where

$$K(x, y) = \frac{L}{4} - \max\{x, y\} + \frac{1}{2}(x + y). \qquad (2.6)$$

Here K is the interaction kernel defined in the square domain $[0, L]\times[0, L]$ (see Figure 2); notice that the scale of interaction is of the order of the size of the domain. The energy functional (2.5) can now be rewritten as

$$\begin{aligned}F(w) &= \int_0^L \big[W(w) + bk(x)w^2 + a|Dw|^2\big]\mathrm{d}x \\ &\quad -\frac{b}{2}\int_0^L \int_0^L K(x, y)\big[w(x) - w(y)\big]^2\mathrm{d}x\,\mathrm{d}y, \qquad (2.7)\end{aligned}$$

where

$$k(x) = \int_0^L K(x, y)\,\mathrm{d}y.$$

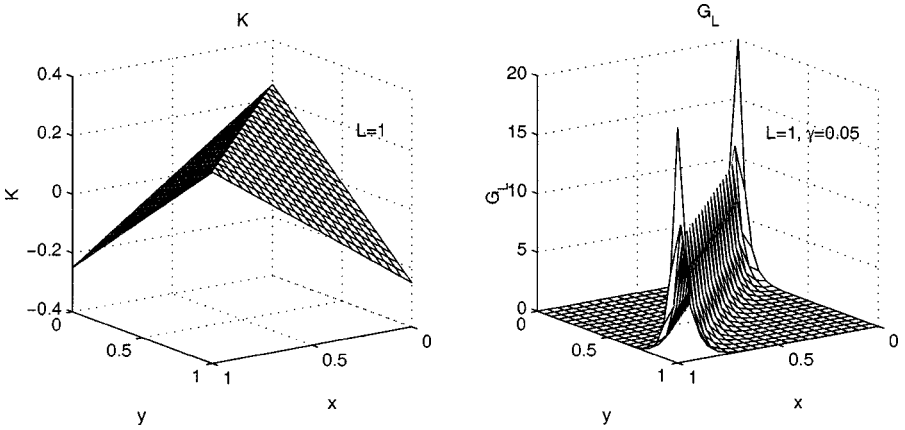

Figure 2. The kernels $K(x, y) = L/4 - \max\{x, y\} + (1/2)(x + y)$ and $G_L(x, y) = 1/(\gamma(e^{L/\gamma} - e^{-L/\gamma}))[\cosh((x + y - L)/\gamma) + \cosh((|x - y| - L)/\gamma)]$.

One can see from Figure 2 that the kernel of the *essentially* nonlocal interaction in (2.7) is negative exactly in the domain where the interaction is the strongest (near the diagonal $x = y$). This observation suggests a general framework for bringing a (non-one-dimensional) microstructure-stabilizing constraint into the semi-quantitative one-dimensional models.

3. The Model

Motivated by the example from the previous section, we consider the following functional:

$$F(w) = \int_0^L \left[W(w) + \frac{\epsilon^2}{2} |Dw|^2 \right] \mathrm{d}x + \frac{1}{4} \int_0^L \int_0^L J(x, y) \big(w(x) - w(y)\big)^2 \mathrm{d}x\, \mathrm{d}y, \tag{3.1}$$

where $J \leqslant 0$. The Euler–Lagrange equation and the natural boundary conditions in this model are

$$\begin{cases} W'(w) - \epsilon^2 D^2 w + \big(jw - J[w]\big) = \sigma, \\ Dw(0) = Dw(L) = 0. \end{cases} \tag{3.2}$$

Here we introduced

$$j(x) = \int_0^L J(x, y)\, \mathrm{d}y \quad \text{and} \quad J[w](x) = \int_0^L J(x, y) w(y)\, \mathrm{d}y.$$

The constant parameter σ, which has a meaning of the overall stress, is to be determined together with the strain field $w(x)$ from the condition (2.2).

Consider a class of exponential kernels of the type $J(x, y) = -\delta G_\infty(|x - y|)$, where

$$G_\infty\big(|x - y|\big) = \frac{1}{2\gamma} e^{-|x-y|/\gamma} \tag{3.3}$$

and $\gamma > 0, \delta > 0$ are constant parameters characterizing the range and the scale of the nonlocal interaction. We notice that $G_\infty(|x - y|)$ is the Green function for the screened Poisson's equation

$$-\gamma^2 D^2 y + y = f$$

defined in the infinite domain $(-\infty, \infty)$. The fact that the kernel $G_\infty(|x - y|)$ is special allows one to reformulate the integro–differential equation (3.2) as a pair of second order differential equations. The corresponding local problem will contain explicit dependence on x (see, for instance, [13, 14]). To make the local problem spatially independent, one has to modify accordingly the kernel $J(x, y)$; it is clear that this modification will only affect the regions near the boundary of the interval $(0, L)$.

In fact, consider a new class of kernels

$$J(x, y) = -\delta G_L(x, y), \tag{3.4}$$

where $G_L(x, y)$ is the Green function for the following boundary value problem on $(0, L)$:

$$\begin{aligned} -\gamma^2 D^2 y + y &= f, \\ Dy(0) = Dy(L) &= 0. \end{aligned}$$

The expression of $G_L(x, y)$ can be given explicitly:

$$G_L(x, y) = \frac{1}{\gamma(e^{L/\gamma} - e^{-L/\gamma})}\left[\cosh\left(\frac{x + y - L}{\gamma}\right) + \cosh\left(\frac{|x - y| - L}{\gamma}\right)\right] \tag{3.5}$$

(see Figure 2). The above class of interaction kernels with a plus sign in (3.4) was previously considered in [27].

To illustrate the relation between $G_L(x, y)$ and $G_\infty(|x - y|)$, we rewrite the kernel $G_L(x, y)$ in the form

$$\begin{aligned} G_L\left(x + \frac{L}{2}, y + \frac{L}{2}\right) &= \frac{1}{2\gamma} e^{-|x-y|/\gamma} + \frac{1}{2\gamma \sinh(L/\gamma)}\left[\cosh\left(\frac{x + y}{\gamma}\right)\right. \\ &\quad \left. + e^{-L/\gamma} \cosh\left(\frac{x - y}{\gamma}\right)\right]. \end{aligned}$$

If we fix points x and y and stretch L, we obtain

$$G_L\left(x + \frac{L}{2}, y + \frac{L}{2}\right) \to G_\infty(x, y) = \frac{1}{2\gamma} e^{-|x-y|/\gamma}$$

which means that in the limit $L \to \infty$ the nonlocal interaction is effectively described by the kernel $G_\infty(|x-y|)$; at finite L the two interactions differ near the boundaries of the domain only.

In what follows we fix the kernel $J(x, y) = -\delta G_L(x, y)$ and formulate the mathematical problem:

MODEL 1. Minimize the functional

$$F^1(w) = \int_0^L \left[W(w) + \frac{\epsilon^2}{2}|Dw|^2 \right] \mathrm{d}x - \frac{\delta}{4}\int_0^L \int_0^L G_L(x, y)\big(w(x) - w(y)\big)^2 \mathrm{d}x\, \mathrm{d}y, \tag{3.6}$$

where w is taken from the set $W^{1,2}(0, L) \cap X$ and

$$X = \left\{ w \in L^2(0, L): \int_0^L w(x)\, \mathrm{d}x = d \right\}. \tag{3.7}$$

The Euler–Lagrange equation and the natural boundary conditions for this problem are

$$\begin{cases} W'(w) - \epsilon^2 D^2 w - \delta\big(w - G_L[w]\big) = \sigma, \\ Dw(0) = Dw(L) = 0, \end{cases} \tag{3.8}$$

where $G_L[w](x) = \int_0^L G_L(x, y)w(y)\, \mathrm{d}y$.

In addition to Model 1 we consider an auxiliary problem:

MODEL 2. Minimize the functional

$$F^2(w) = \int_0^L \left\{ W(w) + \frac{\epsilon^2}{2}|Dw|^2 - \frac{\delta}{2}w^2 + \frac{\delta}{2}\big[\big(-\gamma^2 D^2 + 1\big)^{-1/2} w\big]^2 \right\} \mathrm{d}x, \tag{3.9}$$

where $w \in W^{1,2}(0, L) \cap X$.

The operator $(-\gamma^2 D^2 + 1)^{-1/2}$ is defined as follows. Suppose v is a (unique) solution of the following linear boundary value problem:

$$\big(-\gamma^2 D^2 + 1\big)v = w, \qquad Dv(0) = Dv(L) = 0.$$

Then the action of the operator $(-\gamma^2 D^2 + 1)^{-1/2}$ is defined by

$$\int_0^L \big[\big(-\gamma^2 D^2 + 1\big)^{-1/2} w\big]^2 \mathrm{d}x = \int_0^L vw\, \mathrm{d}x.$$

The Euler–Lagrange equation and the natural boundary conditions in Model 2 can be written as

$$\begin{cases} W'(w) - \epsilon^2 D^2 w - \delta\big[w - \big(-\gamma^2 D^2 + 1\big)^{-1} w\big] = \sigma, \\ Dw(0) = Dw(L) = 0. \end{cases} \tag{3.10}$$

Now introduce the second auxiliary problem:

MODEL 3. Find critical points of

$$F^3(w, v) = \int_0^L \left\{ W(w) + \frac{\epsilon^2}{2}|Dw|^2 - \frac{\delta}{2}\big[(w - v)^2 + \gamma^2 |Dv|^2\big] \right\} \mathrm{d}x, \tag{3.11}$$

where $(w, v) \in (W^{1,2}(0, L) \cap X) \oplus W^{1,2}(0, L)$.

The Euler–Lagrange equations and the natural boundary conditions in this model take the form

$$\begin{cases} W'(w) - \epsilon^2 D^2 w - \delta(w - v) = \sigma, \\ \gamma^2 D^2 v - v = -w, \\ Dw(0) = Dw(L) = 0, \\ Dv(0) = Dv(L) = 0. \end{cases} \tag{3.12}$$

The proposition below establishes the relation among the three models. Let us select a particular critical point (w, v) of F^3 and set

$$\begin{aligned} \mathcal{M}_1 &= \big\{(\tilde{w}, \tilde{v})\colon \tilde{w} \in W^{1,2}(0, L) \cap X,\ \tilde{v} = \big(-\gamma^2 D^2 + 1\big)^{-1} \tilde{w}\big\}, \\ \mathcal{M}_2 &= \big\{(w, \tilde{v})\colon \tilde{v} \in W^{1,2}(0, L)\big\}. \end{aligned}$$

PROPOSITION 3.1. *The models 1, 2 and 3 are equivalent in the following sense:*

1. *For each $w \in W^{1,2}(0, L) \cap X$, $F^1(w) = F^2(w)$.*
2. *The pair (w, v) is a critical point of F^3 iff $w \in W^{1,2}(0, L) \cap X$ is a critical point of F^1 (and F^2) and $v = (-\gamma^2 D^2 + 1)^{-1} w \in W^{1,2}(0, L)$. Moreover, in this case $F^1(w) = F^3(w, v)$.*
3. *If w is a local or global minimum of F^1 in $W^{1,2}(0, L) \cap X$, then (w, v), where $v = (-\gamma^2 D^2 + 1)^{-1} w$, is a saddle point of F^3 in $(W^{1,2}(0, L) \cap X) \oplus W^{1,2}(0, L)$. Moreover, (w, v) is a minimum of F^3 on the manifold $\mathcal{M}_1$, and a maximum of F^3 on the manifold $\mathcal{M}_2$.*

Proof. To prove part 1 of the proposition, we note that

$$\begin{aligned} F^1(w) &= \int_0^L \left[W(w) + \frac{\epsilon^2}{2}|Dw|^2 - \frac{\delta}{2} w^2 \right] \mathrm{d}x \\ &\quad + \frac{\delta}{2} \int_0^L \int_0^L w(x) G_L(x, y) w(y)\, \mathrm{d}x\, \mathrm{d}y. \end{aligned}$$

Here we have used the fact that

$$\int_0^L G_L(x, y)\,\mathrm{d}y = 1$$

for all $x \in (0, 1)$. If we write

$$\int_0^L G_L(x, y)w(y)\,\mathrm{d}y = \left[\left(-\gamma^2 D^2 + 1\right)^{-1} w\right](x),$$

we find

$$\int_0^L \int_0^L w(x)G_L(x, y)w(y)\,\mathrm{d}x\,\mathrm{d}y = \int_0^L w(x)\left[\left(-\gamma^2 D^2 + 1\right)^{-1} w\right](x)\,\mathrm{d}x,$$

and since $(-\gamma^2 D^2 + 1)^{-1}$ is a self-adjoint positive operator, we obtain

$$\int_0^L w(x)\left[\left(-\gamma^2 D^2 + 1\right)^{-1} w\right](x)\,\mathrm{d}x = \int_0^L \left[\left(-\gamma^2 D^2 + 1\right)^{-1/2} w\right]^2 \mathrm{d}x.$$

Here $(-\gamma^2 D^2 + 1)^{-1/2}$ is the positive square root of $(-\gamma^2 D^2 + 1)^{-1}$. Now the functional $F^1(w)$ becomes

$$F^1(w) = \int_0^1 \left\{W(w) + \frac{\epsilon^2}{2}|Dw|^2 - \frac{\delta}{2}w^2 + \frac{\delta}{2}\left[\left(-\gamma^2 D^2 + 1\right)^{-1/2} w\right]^2\right\}\mathrm{d}x,$$

which proves that $F^1(w) = F^2(w)$.

To see part 2 of the proposition, we first compare the Euler–Lagrange equations for the three models and find that they are identical. Now, suppose that for every $w \in W^{1,2}(0, L) \cap X$, v is such that

$$-\gamma^2 D^2 v + v = w, \qquad Dv(0) = Dv(L) = 0.$$

Then

$$F^2(w) = \int_0^L \left\{W(w) + \frac{\epsilon^2}{2}|Dw|^2 - \frac{\delta}{2}w^2 + \frac{\delta}{2}wv\right\}\mathrm{d}x.$$

However

$$\int_0^L [wv]\,\mathrm{d}x = \int_0^L \left[\gamma^2|Dv|^2 + v^2\right]\mathrm{d}x,$$

which can also be rewritten as

$$\int_0^L [wv]\,\mathrm{d}x = \int_0^L \left[-\left(\gamma^2|Dv|^2 + v^2\right) + 2wv\right]\mathrm{d}x.$$

The functional $F^2(w)$ becomes

$$F^2(w) = \int_0^L \left\{W(w) + \frac{\epsilon^2}{2}|Dw|^2 - \frac{\delta}{2}\left[(w - v)^2 + \gamma^2|Dv|^2\right]\right\}\mathrm{d}x,$$

which proves that $F^1(w) = F^2(w) = F^3(w, v)$

To see part 3 of the proposition, we note from part 2 that when $(w, v) \in \mathcal{M}_1$, $F^3(w, v) = F^1(w)$. Therefore, a minimum w of F^1 gives a minimum $(w, v = (-\gamma^2 D^2 + 1)^{-1} w)$ in $\mathcal{M}_1$. In $\mathcal{M}_2$, F^3 is quadratic and concave in $\tilde{v}$, so along this manifold v is the point of global maximum. □

REMARK 3.2. Model 3 describes the equilibrium states in the FitzHugh–Nagumo theory of activator–inhibitor reaction–diffusion systems (e.g, [11]). The internal parameter v can also be considered as an analog of the internal shear in a Timoshenko-like model of a beam with negative (!) bending stiffness (e.g., [27, 30]).

4. Nondimensionalization and Scaling

Our energy functional depends on 4-dimensional parameters ϵ, γ, δ and L. By rescaling the independent variable x, we can reduce this number to three. In fact, introduce $\bar{x} = x/L$ and $\overline{w}(\bar{x}) = w(x)$. Then the functional $\overline{F^2}(\overline{w}) = F^2(w)/L$ can be written as

$$\overline{F^2}(\overline{w}) = \int_0^1 \left\{ W(\overline{w}) + \frac{\bar{\epsilon}^2}{2} |\overline{D}\overline{w}|^2 - \frac{\bar{\delta}}{2}\overline{w}^2 + \frac{\bar{\delta}}{2}\left[\left(-\bar{\gamma}^2 \overline{D}^2 + 1 \right)^{-1/2} \overline{w} \right]^2 \right\} \mathrm{d}\bar{x}, \quad (4.1)$$

where the differential operator $\overline{D}$ is the derivative with respect to $\bar{x}$ and

$$\bar{\epsilon} = \frac{\epsilon}{L}, \qquad \bar{\delta} = \delta, \qquad \bar{\gamma} = \frac{\gamma}{L}$$

are the main non-dimensional parameters of the problem. Two of them, $\bar{\epsilon}$ and $\bar{\delta}$, are direct analogs of the parameters a and b in the model of a bar on an elastic foundation (2.4). Since our nonlocal interaction is a long-range one, we assume that the third parameter $\bar{\gamma} \sim 1$.

Notice, that in the limit $\bar{\epsilon} \to 0$, $\bar{\delta} \to 0$ the energy (4.1) formally converges to (2.1), and in the naive limit we obtain microstructures with unspecified number of interfaces. More careful analysis shows that, as in the case of a bar on an elastic foundation, the asymptotics of the number of interfaces depends on the joint limit of the non-dimensional parameters $\bar{\delta}$ and $\bar{\epsilon}$. Following the arguments presented in [34], one can show that the number of interfaces in the limit $\bar{\epsilon} \to 0$, $\bar{\delta} \to 0$ depends on the ratio $\bar{c} = \bar{\epsilon}^{-1}\bar{\delta}$. If $\bar{c} \sim 1$ the limiting solution will contain a finite number of interacting interfaces, each of width $\sim \bar{\epsilon}$. The fine structure of the phase boundaries is then completely controlled by the gradient term in the energy functional while their long range interaction is determined by the negative definite nonlocal contribution to the energy. With this limit in view, we assume that $\bar{\delta} = \bar{\epsilon}\bar{c}$ and rewrite our functional in the form

$$\begin{aligned} \overline{F}_{\bar{\epsilon}}(\overline{w}) \;=\; & \int_0^1 \left\{ W(\overline{w}) + \frac{\bar{\epsilon}^2}{2} \left| \overline{D}\overline{w} \right|^2 - \frac{\bar{\epsilon}\bar{c}}{2}\overline{w}^2 \right. \\ & \left. + \frac{\bar{\epsilon}\bar{c}}{2}\left[\left(-\bar{\gamma}^2 \overline{D}^2 + 1 \right)^{-1/2} \overline{w} \right]^2 \right\} \mathrm{d}\bar{x}. \end{aligned} \quad (4.2)$$

The constraint (2.2) becomes

$$\int_0^1 \overline{w}(\bar{x})\,\mathrm{d}\bar{x} = \bar{d}, \tag{4.3}$$

where $\bar{d} = d/L$. In the present formulation the only small parameter is $\bar{\epsilon}$ and we focus our analysis on the asymptotics as $\bar{\epsilon} \to 0$. In what follows, we omit the unnecessary overbars.

5. The $\epsilon \to 0$ Limit

As ϵ approaches 0, the minimizer w_ϵ of F_ϵ tends to a minimizer of another variational problem, F_0, the Γ-limit of $\epsilon^{-1}F_\epsilon$ (see [8] for the definition of Γ-convergence). In this section we explicitly describe the limiting problem; the rigorous mathematical proofs are given in the Appendix.

We first observe that because of the continuity of the nonlocal term, the behavior of our system in the limit of small ϵ is similar to the behavior of the corresponding gradient model (2.3). In particular, at $\epsilon \to 0$ the phase boundaries become infinitely sharp, while the displacement gradients inside the phases assume constant values in the bottoms of the energy wells. As a result, the problem reduces to finding the *geometry* of the domain occupied by one of the phases. This, in turn, means finding the corresponding characteristic function. Notice that the strain gradient term drives the system towards the lower "surface area", which means the minimization of the number of interfaces. In terms of the interface interaction this means repulsion and leads to the overall coarsening. Alternatively, the nonlocal term in the energy causes the interfaces to attract each other and produces a tendency towards the refinement.

We begin with the formal introduction of an adequate space for the limiting strain field. To make our analysis slightly more general, we assume that the energy density $W(w)$ has two nonsymmetric wells located at $w = \alpha$ and $w = \beta$. We take $\epsilon^{-1}F_\epsilon$ as a family of functionals defined on $W^{1,2}(0,1) \cap X$, where F_ϵ is given in (4.2).

We say that a function χ is in $BV((0,1),\{\alpha,\beta\}) \cap X$ if for every $x \in (0,1)$, $\chi(x) = \alpha$ or β, and there are finitely many points $x_1, x_2, \ldots, x_N$ in (0,1), where χ jumps between α and β. The jumps describe the phase boundaries whose locations, given by the numbers $x_1, x_2, \ldots, x_N$, remain unknown.

As we show in the Appendix, the family of strain fields w_ϵ in $W^{1,2}(0,1) \cap X$ with the property that $\epsilon^{-1}F_\epsilon(w_\epsilon)$ is bounded uniformly in ϵ converges to a function χ in $BV((0,1),\{\alpha,\beta\}) \cap X$. Moreover, in the original functional

$$\epsilon^{-1}F_\epsilon(w_\epsilon) = \int_0^1 \left\{ \frac{1}{\epsilon}W(w_\epsilon) + \frac{\epsilon}{2}|Dw_\epsilon|^2 - \frac{c}{2}w_\epsilon^2 + \frac{c}{2}\left[\left(-\gamma^2 D^2 + 1\right)^{-1/2} w_\epsilon\right]^2 \right\} \mathrm{d}x,$$

the "gradient" part

$$\int_0^1 \left\{ \frac{1}{\epsilon} W(w_\epsilon) + \frac{\epsilon}{2} |Dw_\epsilon|^2 \right\} \mathrm{d}x$$

Γ-converges to $c_0 N$, where N is the number of the points where χ jumps, and c_0 is defined by

$$c_0 = \sqrt{2} \int_\alpha^\beta \big[W(t)\big]^{1/2} \, \mathrm{d}t, \tag{5.1}$$

(e.g., [21]). The Γ-limit of the "nonlocal" part of the energy,

$$\int_0^1 \left\{ -\frac{c}{2} w_\epsilon^2 + \frac{c}{2} \big[\big(-\gamma^2 D^2 + 1 \big)^{-1/2} w_\epsilon \big]^2 \right\} \mathrm{d}x,$$

turns out to be trivially

$$\int_0^1 \left\{ -\frac{c}{2} \chi^2 + \frac{c}{2} \big[\big(-\gamma^2 D^2 + 1 \big)^{-1/2} \chi \big]^2 \right\} \mathrm{d}x.$$

Although the above integral represents an implicit function of the location of the phase boundaries $x_1, x_2, \ldots, x_N$, the first term can be calculated exactly. In fact, the constraint $\int_0^1 \chi \, \mathrm{d}x = \int_0^1 w_\epsilon \, \mathrm{d}x = d$ implies that the size of the set where $\chi = \alpha$ is $(\beta - d)/(\beta - \alpha)$ and the size of the set where $\chi = \beta$ is $(d - \alpha)/(\beta - \alpha)$. Then

$$\int_0^1 \chi^2 \, \mathrm{d}x = \alpha^2 \frac{\beta - d}{\beta - \alpha} + \beta^2 \frac{d - \alpha}{\beta - \alpha} = (\alpha + \beta) d - \alpha\beta.$$

To summarize, the limiting functional F_0 is defined by

$$\begin{aligned} F_0(\chi) \;=\; & c_0 \mathcal{S}(\chi) + \frac{c}{2} \Bigg\{ -(\alpha + \beta) d + \alpha\beta \\ & + \int_0^1 \big[\big(-\gamma^2 D^2 + 1 \big)^{-1/2} \chi \big]^2 \mathrm{d}x \Bigg\}. \end{aligned} \tag{5.2}$$

The function $\mathcal{S}(\chi) = N$ denotes the number of points where χ jumps. The class of all admissible fields χ can be decomposed into

$$BV\big((0,1), \{\alpha, \beta\}\big) \cap X = \bigcup_{N=1}^{\infty} A_N,$$

where $A_N = \{\chi \in BV((0,1), \{\alpha, \beta\}) \cap X \colon \mathcal{S}(\chi) = N\}$. In other words A_N is the set of functions in $BV((0,1), \{\alpha, \beta\})$ which have N jumps. The spaces A_N can be further decomposed into

$$A_N = A_N^\alpha \cup A_N^\beta,$$

where $A_N^\alpha = \{\chi \in A_N\colon \chi(x) = \alpha, \text{for } x \in (0, x_1)\}$ and $A_N^\beta = \{\chi \in A_N\colon \chi(x) = \beta, \text{for } x \in (0, x_1)\}$. A_N^α is the part of A_N where functions equal α before their jump point x_1, and A_N^β is the rest part of A_N where functions equal β before their first jump point x_1. More specifically, the subspace A_N^α can be identified with

$$\big\{(x_1, x_2, \ldots, x_N) \in \mathbb{R}^N\colon x_1 < x_2 < \cdots < x_N,\ \alpha x_1 + \beta(x_2 - x_1) + \cdots = d\big\},$$

and the subspace A_N^β with

$$\big\{(x_1, x_2, \ldots, x_N) \in \mathbb{R}^N\colon x_1 < x_2 < \cdots < x_N,\ \beta x_1 + \alpha(x_2 - x_1) + \cdots = d\big\}.$$

The minimization of F_0, which turns out to be a problem in a *finite-dimensional* space of an unknown dimension, can be subdivided into two steps. First, we solve a N-dimensional problem in each A_N^α and A_N^β. The minimizer turns out to be unique in each of the subspaces: χ_N^α in A_N^α and χ_N^β in A_N^β. The symmetry between A_N^α and A_N^β is manifested through the fact that $F_0(\chi_N^\alpha) = F_0(\chi_N^\beta)$ (see Proposition 6.3). This allows us to define

$$F_0^*(N) = F_0\big(\chi_N^{\alpha,\beta}\big). \tag{5.3}$$

The second step of our procedure is the *discrete* minimization of $F_0^*(N)$ among all positive integers N.

We present our approach in the form of the following schematic diagram:

$$\begin{aligned}
&\min_w F_\epsilon(w), \quad w \in W^{1,2}(0,1) \cap X,\\
&\Gamma\text{-converge} \xrightarrow{\epsilon\to 0} \min_\chi F_0(\chi), \quad \chi \in BV\big((0,1), \{\alpha, \beta\}\big) \cap X\\
&\qquad\Longrightarrow \left\langle \begin{array}{l} \min\limits_{(x_1,\ldots,x_N)} F_0(x_1, \ldots, x_N),\ (x_1, \ldots, x_N) \in A_N^\alpha \rightsquigarrow \chi_N^\alpha \\ \min\limits_{(x_1,\ldots,x_N)} F_0(x_1, \ldots, x_N),\ (x_1, \ldots, x_N) \in A_N^\beta \rightsquigarrow \chi_N^\beta \end{array} \right\rangle\\
&\qquad\Longrightarrow \min_N F_0^*(N), \quad N \in \{1, 2, \ldots\} \rightsquigarrow \chi_{N_*}^{\alpha,\beta}.
\end{aligned}$$

The Γ-limit of the functional (5.2) is computed in the Appendix. The first step of the minimization procedure is discussed in Section 7, the second step is detailed in Section 8.

We close this section with the computation of the partial derivatives of the implicit function

$$\begin{aligned}
F_0(x_1, \ldots, x_N) \;=\; & c_0 N + \frac{c}{2}\Big\{ -(\alpha + \beta)d + \alpha\beta \\
& + \int_0^1 \big[\big(-\gamma^2 D^2 + 1\big)^{-1/2}\chi\big]^2 \mathrm{d}x \Big\}.
\end{aligned} \tag{5.4}$$

Let χ be an element in A_N^α. Then the nonlocal part of (5.4) can be rewritten as

$$\begin{aligned} H(\chi) &= H(x_1, \dots, x_N) = \int_0^1 \left[\left(-\gamma^2 D^2 + 1\right)^{-1/2} \chi\right]^2 \mathrm{d}x \\ &= \int_0^1 \int_0^1 G_L(x, y)\chi(x)\chi(y)\,\mathrm{d}x\,\mathrm{d}y. \end{aligned}$$

Assuming $v = (-\gamma^2 D^2 + 1)^{-1}\chi$, we compute

$$\begin{aligned} \frac{\partial H}{\partial x_1} &= \frac{\partial}{\partial x_1}\left[\int_0^{x_1} \alpha v\,\mathrm{d}x + \int_{x_1}^{x_2} \beta v\,\mathrm{d}x + \cdots + \int_{x_N}^{L} \begin{pmatrix} \alpha \\ \text{or} \\ \beta \end{pmatrix} v\,\mathrm{d}x\right] \\ &= (\alpha - \beta)v(x_1) + \int_0^1 \chi(x)\frac{\partial v}{\partial x_1}(x)\,\mathrm{d}x. \end{aligned}$$

To find $(\partial v/\partial x_1)(x)$, we note that

$$\begin{aligned} \frac{\partial v}{\partial x_1}(x) &= \frac{\partial}{\partial x_1}\left[\int_0^{x_1} \alpha G_L(x, y)\,\mathrm{d}y + \int_{x_1}^{x_2} \beta G_L(x, y)\,\mathrm{d}y \right. \\ &\qquad \left. + \cdots + \int_{x_N}^{1} \begin{pmatrix} \alpha \\ \text{or} \\ \beta \end{pmatrix} G_L(x, y)\,\mathrm{d}y\right] \\ &= (\alpha - \beta)G_L(x, x_1). \end{aligned}$$

Therefore,

$$\frac{\partial H}{\partial x_1} = (\alpha - \beta)v(x_1) + (\alpha - \beta)\int_0^1 \chi(x)G_L(x, x_1)\,\mathrm{d}x = 2(\alpha - \beta)v(x_1).$$

Repeating a similar argument for the other partial derivatives of H, we deduce

$$\nabla H(x_1, x_2, \dots, x_N) = 2(\alpha - \beta)\begin{pmatrix} v(x_1) \\ -v(x_2) \\ v(x_3) \\ \vdots \\ (-1)^{N+1}v(x_N)) \end{pmatrix}. \tag{5.5}$$

If $\chi \in A_N^\beta$, then

$$\nabla H(x_1, x_2, \dots, x_N) = 2(\beta - \alpha)\begin{pmatrix} v(x_1) \\ -v(x_2) \\ v(x_3) \\ \vdots \\ (-1)^{N+1}v(x_N)) \end{pmatrix}. \tag{5.6}$$

This representation of the derivatives of the energy in the N-dimensional problem will be used in the next section which details the first step of our minimization procedure.

6. Minimizing over $x_1, x_2, \ldots, x_N$

We minimize F_0 in A_N^α and A_N^β separately. Our first result is:

PROPOSITION 6.1. *If χ_N^α minimizes F_0 in A_N^α, then χ_N^α is necessary periodic. More specifically,*

$$\chi_N^\alpha(x) = \begin{cases} \alpha, & x \in \left(0, \dfrac{-d+\beta}{(\beta-\alpha)N}\right), \\ \beta, & x \in \left(\dfrac{-d+\beta}{(\beta-\alpha)N}, \dfrac{d+\beta-2\alpha}{(\beta-\alpha)N}\right), \\ \alpha, & x \in \left(\dfrac{d+\beta-2\alpha}{(\beta-\alpha)N}, \dfrac{-d+3\beta-2\alpha}{(\beta-\alpha)N}\right), \\ \beta, & x \in \left(\dfrac{-d+3\beta-2\alpha}{(\beta-\alpha)N}, \dfrac{d+3\beta-4\alpha}{(\beta-\alpha)N}\right), \\ \alpha, & x \in \left(\dfrac{d+3\beta-4\alpha}{(\beta-\alpha)N}, \dfrac{-d+5\beta-4\alpha}{(\beta-\alpha)N}\right), \\ \beta, & x \in \left(\dfrac{-d+5\beta-4\alpha}{(\beta-\alpha)N}, \dfrac{d+5\beta-6\alpha}{(\beta-\alpha)N}\right), \\ \vdots \end{cases}$$

Also, if χ_N^β minimizes F_0 in A_N^β, then χ_N^β is periodic and

$$\chi_N^\beta(x) = \begin{cases} \beta, & x \in \left(0, \dfrac{d-\alpha}{(\beta-\alpha)N}\right), \\ \alpha, & x \in \left(\dfrac{d-\alpha}{(\beta-\alpha)N}, \dfrac{-d+2\beta-\alpha}{(\beta-\alpha)N}\right), \\ \beta, & x \in \left(\dfrac{-d+2\beta-\alpha}{(\beta-\alpha)N}, \dfrac{d+2\beta-3\alpha}{(\beta-\alpha)N}\right), \\ \alpha, & x \in \left(\dfrac{d+2\beta-3\alpha}{(\beta-\alpha)N}, \dfrac{-d+4\beta-3\alpha}{(\beta-\alpha)N}\right), \\ \beta, & x \in \left(\dfrac{-d+4\beta-3\alpha}{(\beta-\alpha)N}, \dfrac{d+4\beta-5\alpha}{(\beta-\alpha)N}\right), \\ \alpha, & x \in \left(\dfrac{d+4\beta-5\alpha}{(\beta-\alpha)N}, \dfrac{-d+6\beta-5\alpha}{(\beta-\alpha)N}\right), \\ \vdots \end{cases}$$

Proof. First consider A_N^α. We use the method of Lagrange multipliers to accommodate the constraint $\alpha x_1 + \beta(x_2 - x_1) + \cdots = d$. For the characteristic function χ to be a minimizer of (5.4), it is necessary that for some constant σ

$$2(\alpha-\beta)\begin{pmatrix} v(x_1) \\ -v(x_2) \\ v(x_3) \\ \vdots \\ (-1)^{N+1}v(x_N) \end{pmatrix} - \sigma(\alpha-\beta)\begin{pmatrix} 1 \\ -1 \\ 1 \\ \vdots \\ (-1)^{N+1} \end{pmatrix} = \begin{pmatrix} 0 \\ 0 \\ 0 \\ \vdots \\ 0 \end{pmatrix}.$$

This obviously implies

$$v(x_1) = v(x_2) = \cdots = v(x_N). \tag{6.1}$$

In particular, $v(x_1) = v(x_2)$ which means that v is symmetric on (x_1, x_2). The function $v(x)$ in this interval can be calculated explicitly:

$$v(x) = \beta + C\cosh\left(\frac{x - (x_1+x_2)/2}{\gamma}\right),$$

where C is a constant of integration. Notice that $Dv(x_1) = -Dv(x_2)$. Now, by uniqueness and existence theorems for ordinary differential equations,we obtain that v on $(0, x_1)$ is a reflection of v on $(x_2, (x_2 + x_3)/2)$. Also because $Dv(0) = 0$, the length of $(0, x_1)$ is half of that of (x_2, x_3). By repeating this argument one can show that the intervals where $\chi = \alpha$ all have the same length with the exception of $(0, x_1)$ (and $(x_N, 1)$), whose length is only a half of the above length. The same can be concluded for the intervals where $\chi = \beta$, say (x_1, x_2), (x_3, x_4), ...: the length of $(0, x_1)$ is $\beta - d/((\beta-\alpha)N)$; the length of (x_1, x_2) is $2(d-\alpha)/((\beta-\alpha)N)$; and the length of (x_2, x_3) is $2(\beta-d)/((\beta-\alpha)N)$. This gives the desired expression for χ_N^α. A similar argument for A_N^β determines χ_N^β. □

REMARK 6.2. For each $\chi_N^{\alpha,\beta}$, by separating variables, the corresponding $v = (-\gamma^2 D^2 + 1)^{-1}\chi_N^{\alpha,\beta}$ can be calculated from the explicit series

$$v(x) = d + \sum_{k=1}^{\infty}\left[\frac{2\int_0^1 \chi_N^{\alpha.\beta}(x)\cos(k\pi x)\,\mathrm{d}x}{k^2\gamma^2\pi^2+1}\cos(k\pi x)\right].$$

Using Proposition 6.1, we can simplify this to

$$\left(-\gamma^2 D^2 + 1\right)^{-1}\chi_N^\alpha = d + 2\sum_{l=1}^{\infty}\frac{(\beta-\alpha)\sin(((\beta-d)/(\beta-\alpha))l\pi)}{l\pi(l^2N^2\gamma^2\pi^2+1)}\cos(lN\pi x),$$

$$\left(-\gamma^2 D^2 + 1\right)^{-1}\chi_N^\beta = d + 2\sum_{l=1}^{\infty}\frac{(\beta-\alpha)\sin(((d-\alpha)/(\beta-\alpha))l\pi)}{l\pi(l^2N^2\gamma^2\pi^2+1)}\cos(lN\pi x).$$

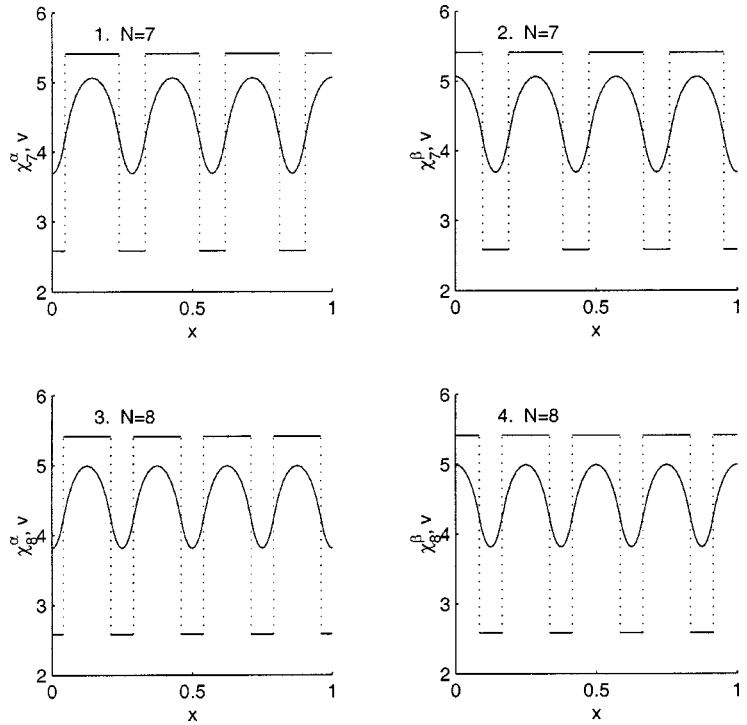

Figure 3. Metastable configurations with $N = 7$ and 8. Shown are the graphs of $\chi_N^{\alpha,\beta}$ and the corresponding $v = (-\gamma^2 D^2 + 1)^{-1}\chi_N^{\alpha,\beta}$. Here $\alpha = 2.59$, $\beta = 5.41$, $d = 4.5$.

Two examples of the functions χ_N^α and χ_N^β and the corresponding functions $v(x)$ are shown in Figure 3. In our numerical calculations we specified

$$W(w) = \left[\frac{1}{4}(w-4)^2 - \frac{1}{2}\right]^2, \tag{6.2}$$

which gives $\alpha = 4 - \sqrt{2}$, $\beta = 4 + \sqrt{2}$. We also choose $d = 4.5$ to be between α and β. In the first two pictures (Figure 3 (1,2)) $N = 7$ (odd), while in the last two pictures (Figure 3 (3,4)) $N = 8$ (even), which illustrate two different morphologies near the boundaries of the domain. Notice that the strains χ_N^α and χ_N^β are discontinuous even when the internal fields v's are smooth.

The next proposition provides an explicit expression for the energy of the minimizer at a given N. The corresponding states are only metastable in the sense of the original problem.

PROPOSITION 6.3.

$$\begin{aligned} F_0^*(N) &= F_0\big(\chi_N^{\alpha,\beta}\big) \\ &= c_0 N - \frac{c(\beta-\alpha)^2\gamma N \sinh\left(\frac{\beta-d}{(\beta-\alpha)\gamma N}\right)\sinh\left(\frac{d-\alpha}{(\beta-\alpha)\gamma N}\right)}{2\sinh\left(\frac{1}{\gamma N}\right)}. \end{aligned}$$

Proof. We will only compute $F_0(\chi_N^\alpha)$ since the computation of $F_0(\chi_N^\beta)$ is identical. We start with

$$\int_0^1 \left[\left(-\gamma^2 D^2+1\right)^{-1/2}\chi_N^\alpha\right]^2 \mathrm{d}x = \int_0^1 \chi_N^\alpha v\,\mathrm{d}x.$$

Here we have used that $v = (-\gamma^2 D^2+1)^{-1}\chi_N^\alpha$. On a subinterval of (0,1), say (a,b), where $\chi_N^\alpha = \alpha$,

$$\begin{aligned}\int_a^b \chi_N^\alpha v &= \alpha\int_a^b v = \alpha\int_a^b \left(\gamma^2 D^2 v+\alpha\right)\\ &= \alpha\gamma^2\big[Dv(b)-Dv(a)\big]+\alpha^2(b-a).\end{aligned}$$

From $\int_0^1 \chi_N^\alpha(x)\,\mathrm{d}x = d$ we find that the measure of the set on which $\chi_N^\alpha = \alpha$ is $(\beta-d)/(\beta-\alpha)$ and the measure of the set on which $\chi_N^\alpha = \beta$ is $(d-\alpha)/(\beta-\alpha)$. Then

$$\begin{aligned}&\int_0^1 \left[\left(-\gamma^2 D^2+1\right)^{-1/2}\chi_N^\alpha\right]^2 \mathrm{d}x\\ &\quad= \alpha^2\frac{\beta-d}{\beta-\alpha}+\beta^2\frac{d-\alpha}{\beta-\alpha}+(\alpha-\beta)\gamma^2\big[Dv(x_1)-Dv(x_2)+Dv(x_3)-\cdots\big]\\ &\quad= (\alpha+\beta)d-\alpha\beta L+(\alpha-\beta)\gamma^2 N Dv(x_1).\end{aligned}$$

Now we need to calculate $Dv(x_1)$. First, observe that on $(0,x_1)$ we have $v(x) = \alpha+C'\cosh(x/\gamma)$ and on (x_1,x_2) we have $v(x) = \beta+C''\cosh((x-(x_1+x_2)/2)/\gamma)$ for some appropriate C' and C''. Both functions as well as their derivatives must match at x_1. Therefore,

$$\begin{cases}\alpha + C'\cosh\left(\dfrac{x_1}{\gamma}\right) = \beta + C''\cosh\left(\dfrac{x_1-x_2}{2\gamma}\right),\\[2ex] \dfrac{C'}{\gamma}\sinh\left(\dfrac{x_1}{\gamma}\right) = \dfrac{C''}{\gamma}\sinh\left(\dfrac{x_1-x_2}{2\gamma}\right).\end{cases}$$

Solving this system we find

$$\begin{cases}C' = \dfrac{(\alpha-\beta)\sinh((x_1-x_2)/(2\gamma))}{\sinh(1/(\gamma N))},\\[2ex] C'' = \dfrac{(\alpha-\beta)\sinh(x_1/\gamma)}{\sinh(1/(\gamma N))}.\end{cases}$$

Recall that

$$x_1 = \frac{\beta-d}{(\beta-\alpha)N}, \qquad x_2-x_1 = \frac{2(d-\alpha)}{(\beta-\alpha)N}, \quad \text{and} \quad \frac{x_1+x_2}{2} = \frac{L}{N}.$$

Then

$$Dv(x_1) = -\frac{(\alpha-\beta)\sinh((\beta-d)/((\beta-\alpha)\gamma N))\sinh((d-\alpha)/((\beta-\alpha)\gamma N))}{\gamma\sinh(1/(\gamma N))}$$

from which we define

$$\int_0^1 \left[\left(-\gamma^2 D^2+1\right)^{-1/2}\chi_N^\alpha\right]^2 \mathrm{d}x$$
$$= (\alpha+\beta)d-\alpha\beta$$
$$-\frac{(\beta-\alpha)^2\gamma N\sinh((\beta-d)/((\beta-\alpha)\gamma N))\sinh((d-\alpha)/((\beta-\alpha)\gamma N))}{\sinh(1/(\gamma N))}.$$

Now the proposition follows from (5.2). □

PROPOSITION 6.4. *χ_N^α minimizes F_0 in A_N^α and χ_N^β minimizes F_0 in A_N^β.*

Proof. Suppose that χ_N^α is not a minimizer of F_0 in A_N^α. Then there exists a sequence $(x_{n,1}, x_{n,2}, \ldots, x_{n,N})$ in $\{(x_1, x_2, \ldots, x_N) \in R^N: x_1 < x_2 < \cdots < x_N, \alpha x_1 + \beta(x_2 - x_1) + \cdots = d\}$ converging to a boundary point and such that

$$\lim_{n\to\infty} H(x_{n,1}, x_{n,2}, \ldots, x_{n,N}) \leqslant H\left(\chi_N^\alpha\right).$$

A boundary point of $\{(x_1, x_2, \ldots, x_N) \in \mathbb{R}^N: x_1 < x_2 < \cdots < x_N, \alpha x_1 + \beta(x_2 - x_1) + \cdots = d\}$ can be considered as a point in $A_{N'}^\alpha$ (or $A_{N'}^\beta$) with $N' < N$. Let us call it $(y_1, y_2, \ldots, y_{N'})$. Now, since $H(\chi_N^{\alpha,\beta})$ decreases in N (see below Proposition 7.1, part 3), we find that $H(y_1, y_2, \ldots, y_{N'}) < H(\chi_{N'}^{\alpha,\beta})$. This implies that either $\chi_{N'}^\alpha$ is not a minimizer in $A_{N'}^\alpha$ or $\chi_{N'}^\beta$ is not a minimizer in $A_{N'}^\beta$. This recursive argument continues until we reach A_1^α (or A_1^β). A contradiction occurs since there is only one element in A_1^α (or A_1^β). □

7. Minimizing over N

The properties of the function $F_0^*(N)$, introduced in Proposition 6.3, are summarized in the following proposition.

PROPOSITION 7.1. *Assume that r takes real values in $(0, \infty)$.*

1. *$F_0^*(r)$ is convex in r.*
2. *$F_0^*(r)$ has the Laurent expansion*

$$F_0^*(r) = c_0 r - \frac{c(\beta-d)(d-\alpha)}{2} + \frac{c(\beta-d)^2(d-\alpha)^2}{6(\beta-\alpha)^2\gamma^2}\frac{1}{r^2} + \cdots.$$

3. *The function*

$$F_0^*(r) - c_0 r = -c(\beta-\alpha)^2\gamma r\sinh\left(\frac{\beta-d}{(\beta-\alpha)\gamma r}\right)\sinh\left(\frac{d-\alpha}{(\beta-\alpha)\gamma r}\right)$$
$$\Big/ 2\sinh\left(\frac{1}{\gamma r}\right),$$

decreases with r.

4. *For large r the curve $F_0^*(r)$ has an asymptote*

$$l(r) = c_0 r - \frac{c(\beta - d)(d - \alpha)}{2}.$$

Proof. Introduce

$$p_1 = \frac{\beta - d}{(\beta - \alpha)\gamma}, \qquad p_2 = \frac{d - \alpha}{(\beta - \alpha)\gamma}.$$

Then

$$\begin{aligned}\frac{\mathrm{d}F_0^*(r)}{\mathrm{d}r} &= c_0 - \frac{c(\beta-\alpha)^2\gamma}{2r(\sinh((p_1+p_2)/r))^2}\left\{ r\sinh\frac{p_1}{r}\sinh\frac{p_2}{r}\sinh\frac{p_1+p_2}{r}\right.\\ &\quad -p_1\cosh\frac{p_1}{r}\sinh\frac{p_2}{r}\sinh\frac{p_1+p_2}{r}\\ &\quad -p_2\sinh\frac{p_1 r}{\cosh}\frac{p_2}{r}\sinh\frac{p_1+p_2}{r}\\ &\quad \left.+(p_1+p_2)\sinh\frac{p_1}{r}\sinh\frac{p_2}{r}\cosh\frac{p_1+p_2}{r}\right\},\end{aligned}$$

and

$$\begin{aligned}\frac{\mathrm{d}^2F_0^*(r)}{\mathrm{d}r^2} &= \frac{c(\beta-\alpha)^2\gamma}{r^3(\sinh 1/(\gamma r))^3}\left\{\cosh\frac{L}{\gamma r}\left[p_1^2\left(\sinh\frac{p_2}{r}\right)^2 + p_2^2\left(\sinh\frac{p_1}{r}\right)^2\right]\right.\\ &\quad \left.-2p_1p_2\sinh\frac{p_1}{r}\sinh\frac{p_2}{r}\right\}.\end{aligned}$$

Now, since $\cosh(1/(\gamma r)) > 1$, we obtain

$$\begin{aligned}\frac{\mathrm{d}^2F_0^*(r)}{\mathrm{d}r^2} &> \frac{c(\beta-\alpha)^2\gamma}{r^3(\sinh 1/(\gamma r))^3}\left\{p_1^2\left(\sinh\frac{p_2}{r}\right)^2 + p_2^2\left(\sinh\frac{p_1}{r}\right)^2\right.\\ &\quad \left.-2p_1p_2\sinh\frac{p_1}{r}\sinh\frac{p_2}{r}\right\} \geqslant 0.\end{aligned}$$

The last inequality implies that the graph of $F_0^*(r)$ versus r is a convex curve. A straightforward calculation gives the Laurent expansion mentioned in the proposition. In particular, it implies

$$\lim_{r\to\infty}\frac{\mathrm{d}F_0^*(r)}{\mathrm{d}r} = c_0.$$

Then the inequality

$$\frac{\mathrm{d}F_0^*(r)}{\mathrm{d}r} < c_0$$

follows from $\mathrm{d}^2F_0^*(r)/\mathrm{d}r^2 > 0$. □

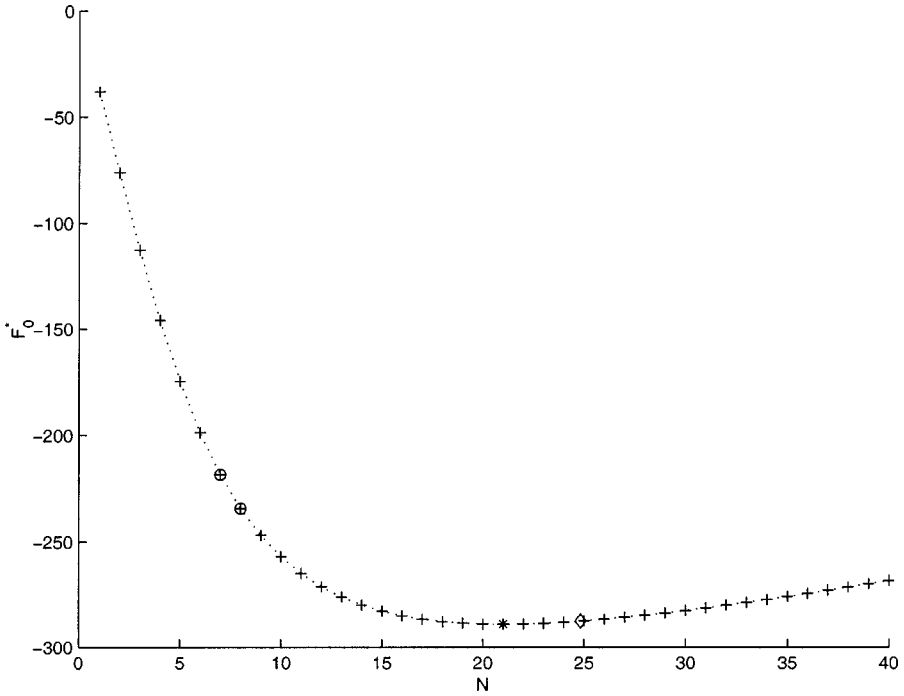

Figure 4. The graph of $F_0^*(N)$ versus N. Here $\alpha = 2.59$, $\beta = 5.41$, $\gamma = 0.05$, $c_0 = 1.33$, $c = 400$ and $d = 4.5$. The markers are explained in the text.

Figure 4 illustrates the behavior of the function $F_0^*(r)$. Here, in addition to the parameters of the energy selected for Figure 3, we choose $\gamma = 0.05$, $c_0 = 4/3$, and $c = 400$. The energies of the four metastable states with $N = 7$ and $N = 8$ (Figure 3) are indicated in Figure 4 by the "cross" markers.

In general, the curve $F_0^*(r)$ versus r, restricted to the interval $[1, \infty)$, has a unique global minimum, say $r = \nu$, where ν is usually not an integer. An integer N_* adjacent to ν minimizes F_0^* among all positive integers. Generically this N_* is unique and there is exactly one pair of global minimizers, $\chi^{\alpha}_{N_*}$ and $\chi^{\beta}_{N_*}$, corresponding to it. It may also happen that for the specific choice of the nondimensional constants there are two consecutive positive integers, N_* and $N_* + 1$, that both minimize $F_0^*(N)$. Then we have two pairs of global minimizers, $\chi^{\alpha}_{N_*}$, $\chi^{\beta}_{N_*}$, $\chi^{\alpha}_{N_*+1}$ and $\chi^{\beta}_{N_*+1}$.

The number N_* can be estimated with the help of the Laurent expansion calculated in part 2 of Proposition 6.3. It follows that

$$N_* \approx \left(\frac{c(\beta - d)^2(d - \alpha)^2}{3c_0(\beta - \alpha)^2\gamma^2} \right)^{1/3}. \tag{7.1}$$

In the example shown in Figure 4, this gives an estimate $N_* \approx 24.8\ldots$, shown as the "diamond" marker, while the exact minimum in the space of integers is

achieved at $N_* = 21$ (indicated with the "star" marker). The agreement obviously improves with increasing c.

Finally, it is instructive to present a dimensional form of (7.1):

$$\frac{N_*}{L} \approx \left(\frac{c(\beta - d/L)^2 (d/L - \alpha)^2}{3c_0(\beta - \alpha)^2 \gamma^2} \right)^{1/3}. \tag{7.2}$$

This expression provides an estimate of the actual number of interfaces per unit length as a function of the average strain and other parameters of the model. Notice that the density of the interfaces does not depend on the size of the body.

8. Dynamics

In the previous sections we studied the structure of the global minimizer in the the variational problem (4.2), (4.3) in the limit $\epsilon \to 0$. To check whether our mechanical system can actually reach the corresponding configuration we need to consider a dynamical extension of the variational problem.

There are two major requirements. The dynamical model should be capable of describing fast processes such as nucleation and (explosive) growth of the microstructure. This requires consideration of the kinetic energy and inclusion of inertial terms into the governing equations. On the other hand, the model must be compatible with the final stabilization of the equilibrium microstructure through the much slower processes of coarsening or refinement of the elastic domains. The description of these phenomena requires the introduction of an adequate dissipative mechanism.

In this section we consider a particular dynamic counterpart of our variational model which introduces both inertia and dissipation in a simple way. To avoid integral equations, we consider a dynamical extension of the local model (Model 3, see (3.11) and (3.12)). In this case we need a system of partial differential equations governing the evolution of the strain field $w(x, t)$ and of an additional field of internal variable $v(x, t)$. We assume that the strain field $w(x, t)$ satisfies the equations of classical inertial visco-elastodynamics. For simplicity, the adjustment of the internal variable $v(x, t)$ is considered instantaneous and the corresponding field inertia-free: in the framework of FitzHugh–Nagumo dynamics this case is known as the fast-inhibitor limit. As we show below, the resulting model represents a nonlocal generalization of the viscosity–capillarity model of Truskinovsky [31] and Slemrod [29].

We begin with an introduction of a displacement field

$$u(x, t) = \int_0^x w(y, t)\, \mathrm{d}y. \tag{8.1}$$

By adding into the Lagrangian a standard kinetic energy associated with the displacement field $u(x,t)$ and assuming the reference mass density to be equal to unity we obtain a system of (dimensional) equations:

$$\begin{cases} u_{tt} = D\big[-\epsilon^2 D^3 u - \delta(Du - v) + W'(Du)\big] + \eta D^2 u_t \\ -\gamma^2 D^2 v + v = Du. \end{cases} \tag{8.2}$$

Here $\eta > 0$ is a constant (Kelvin) viscosity. The initial and boundary conditions for the system (8.2) take the form

$$\begin{cases} u(x,0) = u_0(x), & x \in (0,L), \\ u_t(x,0) = u_1(x), & x \in (0,L), \\ u(0,t) = 0, \quad u(L,t) = d, & t \in (0,T), \\ D^2u(0,t) = D^2u(0,L) = 0, & t \in (0,T), \\ Dv(0,t) = Dv(L,t) = 0, & t \in (0,T). \end{cases} \tag{8.3}$$

When all small parameters δ, γ, η, and ϵ are equal to zero we obtain a mixed type nonlinear wave equation and the problem is ill-posed, which results in a dramatic lack of uniqueness. Partial regularization can be achieved if either $\delta = 0$ or $\gamma = 0$. In this case the (well-posed) model (8.2), (8.3) reduces to the viscosity–capillarity model which is rich enough to describe propagation of isolated shock waves and phase boundaries (e.g., [32]), but is incompatible with nucleation and spreading of the finite scale microstructures. In this sense the full system (8.2) is expected to have a completely new set of solutions comparing to straightforward dispersive and dissipative regularizations of the nonlinear wave equation.

The detailed analysis of the dynamical equations (8.2), (8.3) is beyond the scope of the present paper. In the next section we present some numerical results pertinent to the accessibility of the periodic minimizer.

In our numerical solution of equation (8.2), we choose an *explicit* scheme. Namely, we replace (8.2) with the iteration

$$\begin{aligned} u(x,t+\Delta t) \approx\ & u(x,t) + u_t(x,t)\Delta t + \frac{1}{2}\big\{D\big[-\epsilon^2 D^3 u(x,t) \\ & - \delta\big(Du(x,t) - v(x,t)\big) + W'\big(Du(x,t)\big)\big] \\ & + \eta D^2 u_t(x,t)\big\}\Delta t^2, \end{aligned}$$

where $v(x,t)$ is obtained at each time step by solving the boundary value problem

$$-\gamma^2 D^2 v(x,t) + v(x,t) = Du(x,t), \qquad Dv(0,t) = Dv(1,t) = 0$$

numerically.

9. Computational Results

The goal of this section is to illustrate numerically the generation and stabilization of the microstructures. Specifically, we shall follow the evolution of two sets

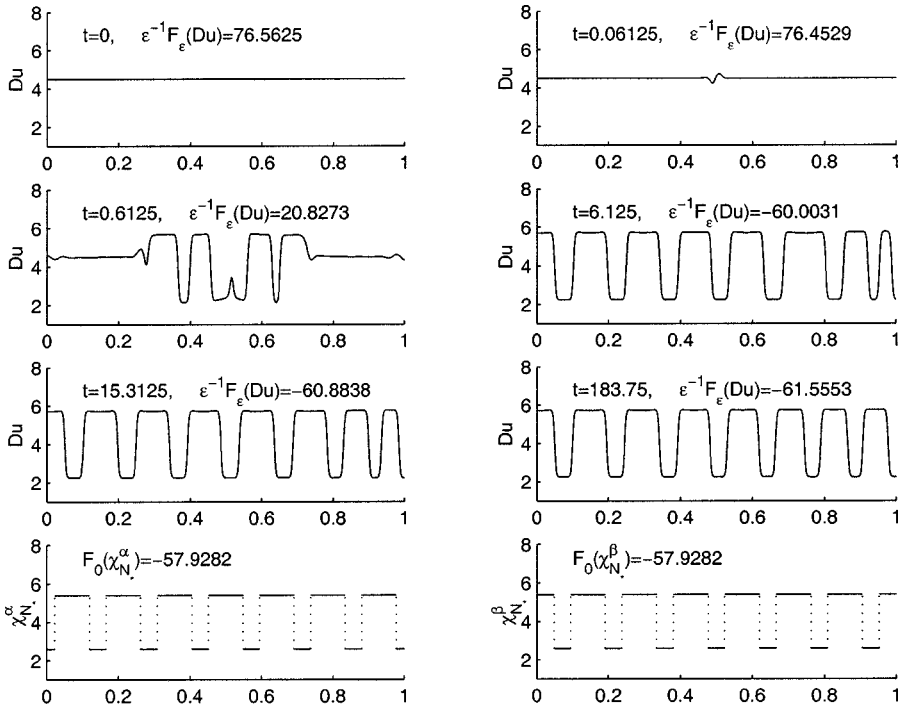

Figure 5. The first six pictures show the evolution of the strain field Du under equations (8.2) and (8.3) at six different times. Here $L = 1$, $d = 4.5$, $\gamma = 0.05$, $\eta = 0.01$, $\epsilon = 0.0025$, $\delta = 0.25$ and $c = 100$. The last two pictures present the minima $\chi^{\alpha}_{N_*}$ and $\chi^{\beta}_{N_*}$ of F_0. The energy density $W$is given by (6.2) with $\alpha = 2.59$, $\beta = 5.41$. In this case $N_* = 14$.

of initial data representing the breakdown of a metastable and an unstable state. The main question is whether the global minimizer is dynamically accessible or whether the system, governed by (8.2), (8.3) get, stuck in a metastable configuration. We remark that the minimizer is known only in the limiting case $\epsilon = 0$ while the calculations are performed at finite ϵ.

In the first set of computations we consider the case when ϵ is sufficiently small so that the functional F_ϵ can be adequately approximated by F_0. Thus, choose $L = 1$, $d = 4.5$, $\gamma = 0.05$, $\eta = 0.01$, $\epsilon = 0.0025$, $\delta = \epsilon c = 0.25$ and $c = 100$. The double well potential W is taken from (6.2).

Suppose initially $u_0(x) = 4.5x$, which corresponds to a uniform metastable strain field, and assume that the localized perturbation of the velocity $u_1(x)$ is small. The initial perturbation must be sufficiently strong to break the metastability. Figure 5 traces the evolution of the strain u_x at six different times t. We observe the nucleation of the microstructure which is followed by its propagation into the undisturbed area. When the growing microstructure reaches the boundary of the domain the process of coarsening begins which eventually leads to an almost periodic pattern. The observed stabilization of the microstructure at large t may mean

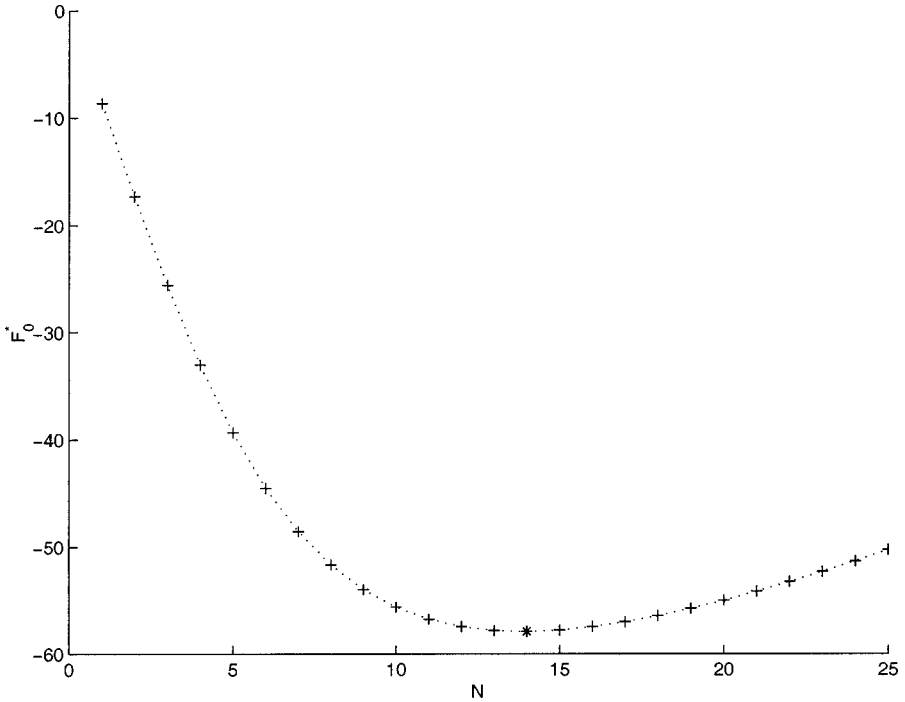

Figure 6. The dependence of F_0^* on N. Here $\alpha = 2.59$, $\beta = 5.41$, $\gamma = 0.05$, $c_0 = 1.33$, $c = 100$ and $d = 4.5$. Note $N_* = 14$.

that the system has reached a state of local/global minimum of the energy. It may also mean significant slowing down in the vicinity of a saddle point.

In order to check different possibilities we can compare the large t configuration with the microstructure delivering the global minimum to the functional F_0. In our case

$$c_0 = \sqrt{2}\int_\alpha^\beta \big[W(t)\big]^{1/2}\mathrm{d}t = \sqrt{2}\int_{4-\sqrt{2}}^{4+\sqrt{2}} \left[\frac{1}{2} - \frac{1}{4}(t-4)^2\right]\mathrm{d}t = \frac{4}{3}.$$

The dependence of $F_0^*(N)$ on N is shown in Figure 6. It is not hard to see that the minimum value of $F_0^*(N)$ is achieved at $N_* = 14$, indicated with the "star" marker. This number agrees quite well with the final picture in Figure 5 where at large t, we observe 15 jumps of u_x. The last two pictures in Figure 5 depict the minimizers $\chi^\alpha_{N_*}$ and $\chi^\beta_{N_*}$ of F_0. In spite of the discrepancy near the boundary, the general agreement between these pictures confirms that the numerical solution is quite close to the global minimizer.

We have also compared the energy $\epsilon^{-1}F_\epsilon(Du)$, calculated from (4.2), with the minimum energy $F_0(\chi^\alpha_{N_*})$ $(= F_0(\chi^\beta_{N_*}))$, explicitly calculated in Proposition 6.3. These numbers are given together with the corresponding Du, $\chi^\alpha_{N_*}$ and $\chi^\beta_{N_*}$ in Figure 5. We find that they match quite well at large t.

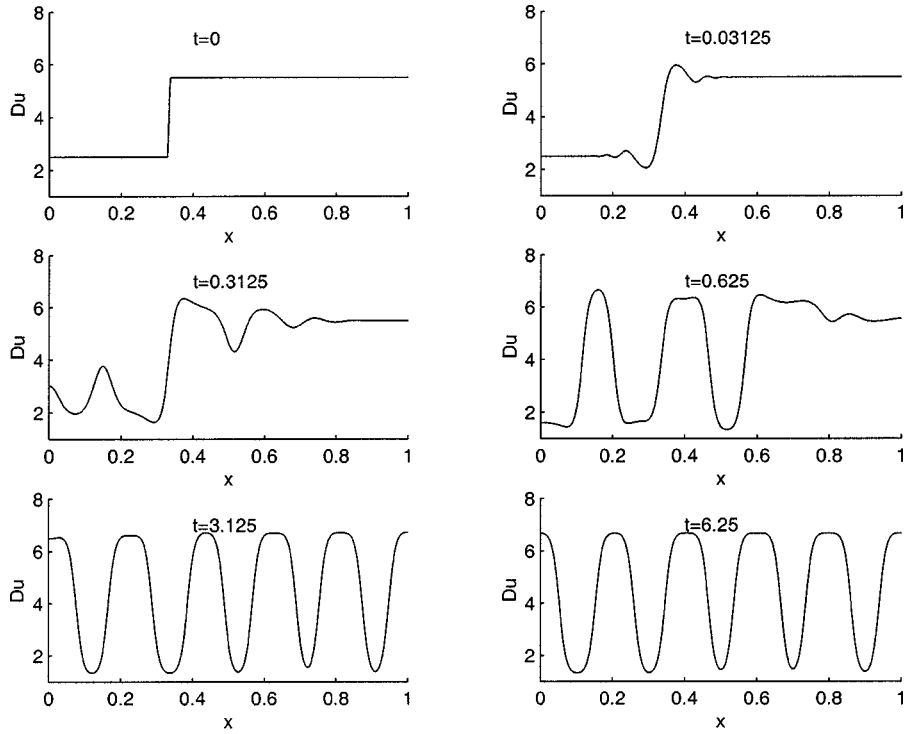

Figure 7. The evolution of the strain field Du at $\epsilon = 0.02$. The rest of the parameters are the same as in Figure 5.

In the second set of computations based on (8.2), (8.3) we use the same parameters except for the higher value of $\epsilon = 0.02$; here we expect a somewhat larger discrepancy with the results of the $\epsilon = 0$ theory. In addition, we change the initial data for $u(x, 0)$, making the configuration unstable, and assuming $u_t(x, 0) = 0$. Specifically we consider a special Riemann problem, when two homogeneous configurations are separated by a sharp interface:

$$u(x,0) = \begin{cases} 2.5x & \text{if } 0 < x \leqslant 1/3, \\ 5.5(x-1) + 4.5 & \text{if } 1/3 \leqslant x < 1. \end{cases}$$

Notice that we preserve the same total elongation d as in the previous set of computations. The corresponding Du is depicted in the first plot of Figure 7.

From the static problem it is quite clear that the above Riemann data are unstable. As a result, the dynamical process begins without any initial perturbation of velocity. First, the shock waves are emitted and the single layer quickly develops into multiple layers. The oscillatory state then propagates in both directions. After the microstructure hits the boundaries, the process of stabilization and coarsening begins. The final pattern is again almost periodic. The interfaces are more diffuse now because of the larger value of ϵ. The count of the number of interfaces suggests

that the achieved microstructure is at most metastable in the sense of the $\epsilon = 0$ limit.

10. Model Allowing for Sharp Interfaces

Although our simple one-dimensional model encompasses all necessary physical ingredients and produces qualitatively reasonable results, it has the problem common to all gradient models which use strain as an order parameter: misrepresentation of the dispersion relations for lattices which leads to over-regularized, unrealistically diffuse interfaces. In fact the typical TEM observations show that the phase or twin boundaries are often close to being atomically sharp. In order to overcome this difficulty, one can try to modify the "surface energy" part of our model and substitute the strain gradient term by a nonlocal term with a *positive* definite kernel. It is known that depending on the parameters of the kernel and the degree of the nonconvexity of the elastic energy, the "positive" nonlocal model can produce both sharp and diffuse interfaces (see, for instance, [3, 12–14]).

In this section we exploit this idea and briefly sketch a variant of the theory which can produce finite scale microstructures with sharp interfaces. Essentially, we combine positive and negative definite nonlocal terms into one sign-indefinite kernel $J(x, y)$. We assume that when x is close to y, the kernel $J(x, y)$ is positive, and when x is away from y, the kernel $J(x, y)$ is negative. Our new energy functional takes the form

$$F(w) = \int_0^1 W(w)\,\mathrm{d}x + \frac{1}{4}\int_0^1\int_0^1 J(x, y)\big(w(x) - w(y)\big)^2\,\mathrm{d}x\,\mathrm{d}y, \qquad (10.1)$$

where

$$J(x, y) = \delta_1 G_1(x, y) - \delta_2 G_2(x, y). \qquad (10.2)$$

The functions G_i are selected as Green functions of the two auxiliary problems

$$-\gamma_i^2 D^2 y + y = f \quad \text{in } (0, 1), \qquad Dy(0) = Dy(1) = 0$$

(see the explicit expression in (3.5)). Notice that $G_1(x, y)$ and $G_2(x, y)$ enter the kernel $J(x, y)$ with different signs; the representative graph of $J(x, y)$ is shown in Figure 8.

By choosing again the kernel to be exponential we are aiming at the equivalent local theory: a blend of the Timoshenko model considered by Rogers and Truskinovsky [27] and the FitzHugh–Nagumo model considered in this paper. In addition to the conventional strain field, the present theory contains two (!) new physical fields.

In order to rewrite the problem as local we introduce two internal variables,

$$p(x) = \int_0^1 G_1(x, y)w(y)\,\mathrm{d}y, \qquad q(x) = \int_0^1 G_2(x, y)w(y)\,\mathrm{d}y. \qquad (10.3)$$

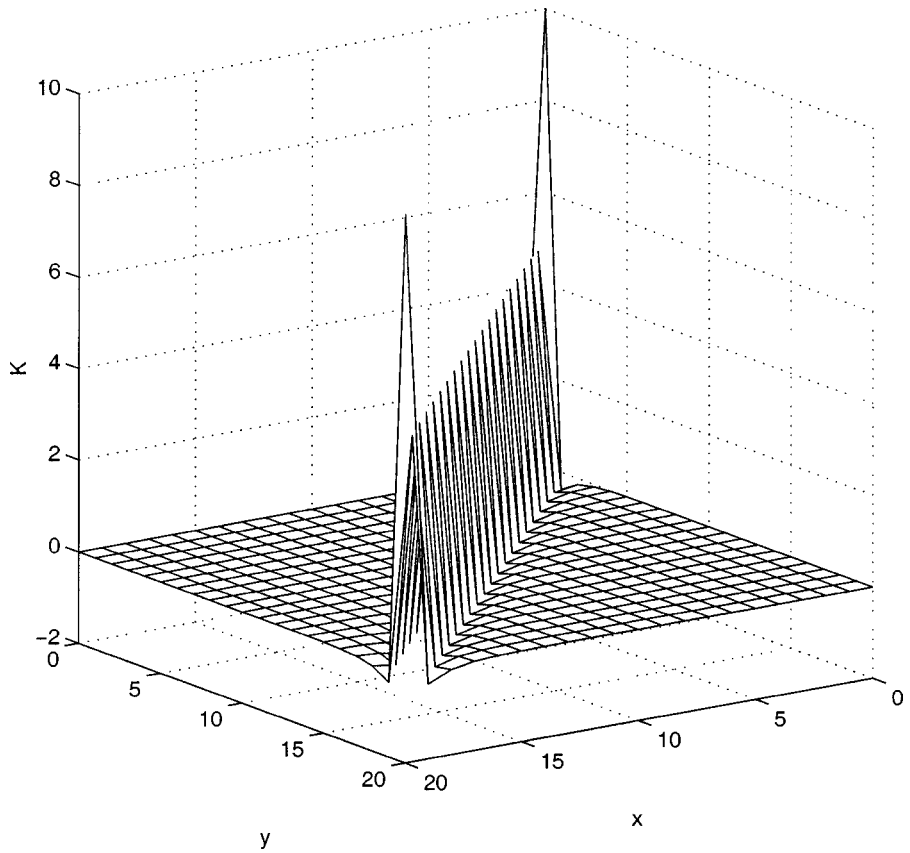

Figure 8. The representative graph of the sign-indefinite kernel $J = \delta_1 G_1 - \delta_2 G_2$ from (10.2). Here $\delta_1 = 1.0$, $\delta_2 = 1.0$, $\gamma_1 = 0.005$ and $\gamma_2 = 0.05$.

In terms of these new variables, the energy functional (3.11) takes the form

$$F^3(w, p, q) = \int_0^1 \left\{ W(w) + \frac{\delta_1 \gamma_1^2}{2} |Dp|^2 + \frac{\delta_1}{2}(p - w)^2 - \frac{\delta_2 \gamma_2^2}{2} |Dq|^2 - \frac{\delta_2}{2}(q - w)^2 \right\} \mathrm{d}x. \tag{10.4}$$

The derivation is identical to the one given in Section 3. Notice that the classical Ericksen's double well energy density is the only nonlinear term in the energy functional. The conventional strain field is linearly coupled with two additional fields, $p(x)$ and $q(x)$, which satisfy linear "field" equations. The Euler–Lagrange equations for this model and the corresponding natural boundary conditions take the forms

$$\begin{cases} \delta_1(w - p) - \delta_2(w - q) + W'(w) = \sigma, \\ -\gamma_1^2 D^2 p + p = w, \qquad Dp(0) = Dp(1) = 0, \\ -\gamma_2^2 D^2 q + q = w, \qquad Dq(0) = Dq(1) = 0. \end{cases} \tag{10.5}$$

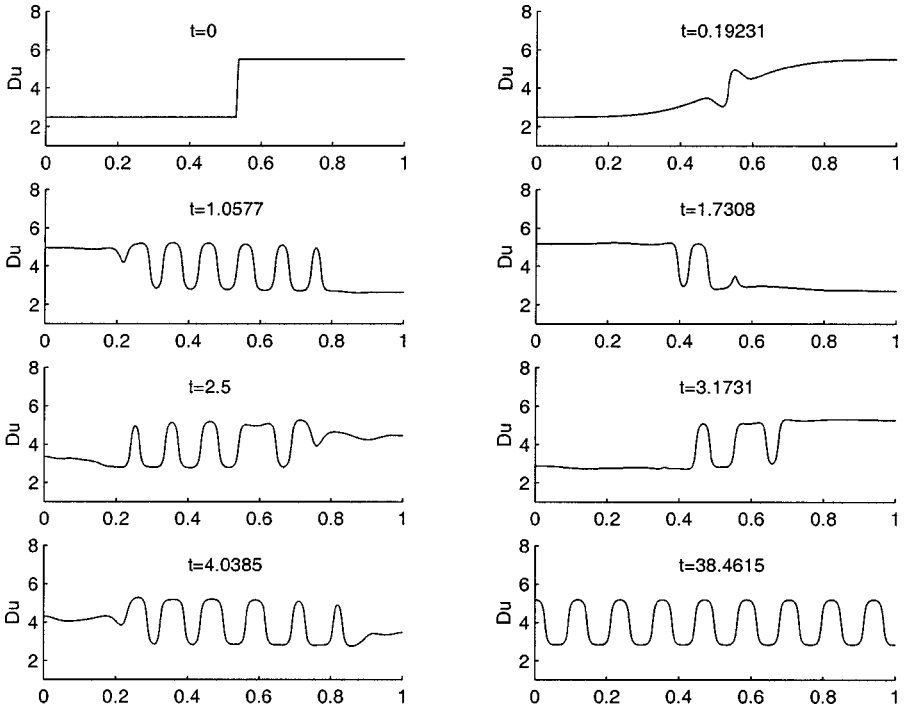

Figure 9. The evolution of the strain field Du according to (10.6). Here $\eta = 0.015$, $d = 3.9$, $\delta_1 = 1.0$, $\delta_2 = 1.0$, $\gamma_1 = 0.005$ and $\gamma_2 = 0.05$.

The detailed analysis of this model will be given elsewhere. Our preliminary results indicate that the new model exhibits periodic minimizers with sharp interfaces.

In dynamics the above model shows interesting reversible transformations between the twinned "martensite" and the surrounding "austenite".

To illustrate this point, consider the simplest dynamic counterpart of (10.1):

$$u_{tt} = D\left[W'(Du) + \int_0^1 J(x,y)\Big(Du(x,t) - Du(y,t)\Big)\mathrm{d}y\right] + \eta D^2 u_t, \tag{10.6}$$

where again $u(x,t) = \int_0^x w(y,t)\,\mathrm{d}y$ is the displacement field. Equation (10.6) is subject to the initial and boundary conditions

$$\begin{cases} u(x,0) = u_0(x), \\ u_t(x,0) = u_1(x), \\ u(0,t) = 0, \qquad u(1,t) = d. \end{cases} \tag{10.7}$$

The dynamical problem (10.6) can also be rewritten in the local form

$$\begin{cases} u_{tt} = D\big[\delta_1(Du - p) - \delta_2(Du - q) + W'(Du)\big] + \eta D^2 u_t, \\ -\gamma_1^2 D^2 p + p = Du, \\ -\gamma_2^2 D^2 q + q = Du. \end{cases} \tag{10.8}$$

The additional boundary conditions for p and q are

$$\begin{cases} Dp(0,t) = Dp(1,t) = 0, \\ Dq(0,t) = Dq(1,t) = 0. \end{cases} \tag{10.9}$$

The results of the numerical simulation of equation (10.1) are shown in Figure 9. We took $\eta = 0.015$, $d = 3.9$ and chose the kernel $J(x, y)$ as in (10.2) with $\delta_1 = 1.0$, $\delta_2 = 1.0$, $\gamma_1 = 0.005$ and $\gamma_2 = 0.05$. In the simulation we start with the unstable Riemann data for Du and zero velocity. We observe that the single interface again develops into multiple layers. The oscillatory state propagates in both direction with clearly indicated fronts; these fronts simulate martensite–austenite interfaces. We observe that the "martensitic" domains behind the moving transition zone are almost stationary so the attractor is not a travelling wave. At some point the layered configuration fills the whole domain. Then the domains near the boundaries start to disappear and the uniform states propagate back but in a reversed order. This process, however, does not go all the way back to the configuration with a single interface. Instead, long before the number of domains reduces to one, the oscillations of the strain field Du start to grow again, propagating towards the boundary. After several repetitions, each time with more "leftover" oscillations, the configuration finally stabilizes, forming a periodic pattern. In the interim period the oscillatory state clearly behaves like an elastic "phase".

11. Conclusions

In this paper we introduced an easily tractable one-dimensional model describing stable finite scale microstructures. This model can be viewed as a one-dimensional ansatz, which in the simplest qualitative form reproduces most of the relevant effects of the full 2- and 3-dimensional formulations. To make a model amenable to analysis we specified the kernel of a nonlocal part of the interaction to be exponential; the more realistic power law kernels can presently be studied numerically at most. We investigated in some detail the important special case when the internal length scales associated with the coarsening and the refinement mechanisms can be separated. By sacrificing some of the metastable configurations, we focused on the asymptotic description of the global minimum. The corresponding limiting problem turned out to be finite-dimensional. We showed that this new problem has a periodic minimizer and explicitly calculated the optimal period. We then looked at the accessibility of the corresponding configuration from the perspective of a realistic dynamics. In particular, we demonstrated how the periodic microstructure nucleates, spreads into the metastable areas and stabilizes. Among other things, we examined the process of final coarsening leading to the microstructure with the predicted period. Our solution presents a new self-consistent description of a moving interface between a homogenous state and a two-phase mixture.

The main open problems are associated with the direct derivation of the nonlocal kernel from the 3-dimensional theory, with the careful analysis of the local

minimizers outside the range of the Γ-limit technique, and with the homogenized description of the kinetics of the propagating microstructures.

Acknowledgments

We thank the reviewer for helpful comments. This work was initiated during the stay of XR as a postdoctoral fellow in the IMA, University of Minnesota. Both authors acknowledge the hospitality of the University of Padova, Italy, in the Fall of 1997.

Appendix

We begin with several technical definitions. Define the set

$$X = \left\{ w \in L^2(0,1) \colon \int_0^1 w(x)\,\mathrm{d}x = d \right\}.$$

The distance between two elements w_1 and w_2 is assumed to be $\|w_1 - w_2\|_{L^2(0,1)}$. We extend the domain of F_ϵ to X by setting $F_\epsilon(w) = \infty$ if $w \in X \backslash W^{1,2}(0,1)$, and the domain of F_0 to X by setting $F_0(\chi) = \infty$ if $\chi \in X \backslash BV((0,1), \{\alpha, \beta\})$. We introduce $BV((0,1), \{\alpha, \beta\})$ as a subset of the space of functions of bounded variation, $BV(0,1)$ (see, for instance, [10, Chapter 5]). A function χ of bounded variation is in $BV((0,1), \{\alpha, \beta\})$ if, for every $x \in (0,1)$, $\chi(x) = \alpha$ or β.

Suppose that the energy density W has two global minima at α and β, i.e., $W(t) \geqslant 0$ and $W(t) = 0$ if and only if $t = \alpha$ or β. We also assume for the technical reasons that W is continuous and there exist $k \geqslant 2$, $K_1 > 0$, $K_2 > 0$, and $\bar{t} > 1$ such that, for all t, $|t| > \bar{t}$,

$$K_1 |t|^k \leqslant W(t) \leqslant K_2 |t|^k. \tag{A.1}$$

We first observe that $\epsilon^{-1} F_\epsilon$ is uniformly bounded below for small ϵ. In fact, for $C > \max\{|\alpha|, |\beta|\}$, and $|w| > C$, we have $(1/\epsilon)W(w) - (c/2)w^2 > 0$ for small ϵ. Then

$$\begin{aligned}
\epsilon^{-1} F_\epsilon(w) &\geqslant \int_0^1 \left[\frac{1}{\epsilon} W(w) - \frac{c}{2} w^2 \right] \mathrm{d}x \\
&\geqslant \int_{\{x : |w(x)| \leqslant C\}} \left[\frac{1}{\epsilon} W(w) - \frac{c}{2} w^2 \right] \mathrm{d}x \\
&\geqslant \int_{\{x : |w(x)| \leqslant C\}} -\frac{c}{2} w^2 \,\mathrm{d}x \geqslant -\frac{cC^2}{2}.
\end{aligned}$$

The relation between $\epsilon^{-1} F_\epsilon$ and F_0 is described here in the language of Γ-convergence, defined as follows (see [8]).

DEFINITION A.1. $\epsilon^{-1}F_\epsilon$ Γ-converges to F_0 if the following two statements hold:

1. For every family $\{w_\epsilon\} \subset X$ with $\lim_{\epsilon\to 0} w_\epsilon = w$,

$$\liminf_{\epsilon\to 0} \epsilon^{-1}F_\epsilon(w_\epsilon) \geqslant F_0(w).$$

2. For every $w \in X \cap BV((0,1),\{\alpha,\beta\})$, there exists a family $\{w_\epsilon\} \subset X$ such that $\lim_{\epsilon\to 0} w_\epsilon = w$ and

$$\limsup_{\epsilon\to 0} \epsilon^{-1}F_\epsilon(w_\epsilon) \leqslant F_0(w).$$

Our first key result is the following proposition.

PROPOSITION A.2. $\epsilon^{-1}F_\epsilon$ Γ-*converges to* F_0.

Proof. For every $w \in X$, we define

$$E_\epsilon(w) = \begin{cases} \displaystyle\int_0^L \left\{\frac{1}{\epsilon}W(w) + \frac{\epsilon}{2}|Dw|^2\right\}\mathrm{d}x & \text{if } w \in W^{1,2}(0,L), \\ \infty & \text{otherwise,} \end{cases} \tag{A.2}$$

$$E_0(w) = \begin{cases} c_0 \mathcal{J}(w) & \text{if } w \in BV((0,L),\{\alpha,\beta\}), \\ \infty & \text{otherwise,} \end{cases} \tag{A.3}$$

and

$$G_L(w) = \int_0^L \left\{ -\frac{c}{2}w^2 + \frac{c}{2}\left[\left(-\gamma^2 D^2 + 1\right)^{-1/2} w\right]^2\right\}\mathrm{d}x. \tag{A.4}$$

It is proved by Modica [21], that E_ϵ Γ-converges to E_0 (with a slight change from $L^1(\Omega)$ to $L^2(0,1)$). The convergence is carried over to $\epsilon^{-1}F_\epsilon \to F_0$ by the continuity of G from X to R. □

Proposition A.2 does not immediately relate the minimizers of $\epsilon^{-1}F_\epsilon$ to the minimizers of F_0. To see the relation we first need a technical lemma.

LEMMA A.3. *Let* $\{\epsilon_n\}$ *be a sequence of positive numbers converging to* 0, *and* $\{w_n\}$ *a sequence of functions in* X. *If* $\epsilon_n^{-1}F_{\epsilon_n}(w_n)$ *is bounded above in* n, *then the sequence* $\{w_n\}$ *is relatively compact in* X *and its cluster points belong to* $BV((0,1),\{\alpha,\beta\})$.

Proof. We set

$$\phi(t) = \int_\alpha^t W^{1/2}(s)\,\mathrm{d}s. \tag{A.5}$$

Then (A.1) implies

$$\left|\phi(t)\right| \leqslant C + C|t|^{k/2+1}.$$

Set $v_n = \phi(w_n)$. By (A.1) and $k \geqslant 2$, we find,

$$|v_n| \leqslant C + C|w_n|^{k/2+1} \leqslant C + CW(w_n).$$

Following the above proof of the uniform lower bound for $\epsilon^{-1}F_\epsilon$, we obtain

$$\begin{aligned}
\epsilon_n^{-1}F_{\epsilon_n}(w_n) &\geqslant \int_0^1 \left[\frac{1}{\epsilon_n}W(w_n) - \frac{c}{2}w_n^2\right]\mathrm{d}x \\
&= \frac{1}{2\epsilon_n}\int_0^1 W(w_n)\,\mathrm{d}x + \int_0^1 \left[\frac{1}{2\epsilon_n}W(w_n) - \frac{c}{2}w_n^2\right]\mathrm{d}x \\
&\geqslant \frac{1}{2\epsilon_n}\int_0^1 W(w_n)\,\mathrm{d}x - \frac{cC^2}{2}.
\end{aligned}$$

Or, in other words,

$$\int_0^1 W(w_n)\,\mathrm{d}x \leqslant 2F_{\epsilon_n}(w_n) + cC^2\epsilon_n, \tag{A.6}$$

which means that $\{v_n\}$ is bounded in $L^1(0,1)$.

On the other hand,

$$\begin{aligned}
\epsilon_n^{-1}F_{\epsilon_n}(w_n) &\geqslant \frac{1}{2}\int_0^1 \left[\epsilon_n|Dw_n|^2 + \frac{1}{\epsilon_n}W(w_n)\right]\mathrm{d}x \\
&\quad + \int_0^1 \frac{1}{2\epsilon_n}\left[W(w_n) - \frac{c}{2}w_n^2\right]\mathrm{d}x \\
&\geqslant \int_0^1 \big(W(w_n)\big)^{1/2}|Dw_n|\,\mathrm{d}x + \int_0^1 \frac{1}{2\epsilon_n}\left[W(w_n) - \frac{c}{2}w_n^2\right]\mathrm{d}x \\
&\geqslant \frac{1}{\sqrt{2}}\int_0^1 |Dv_n|\,\mathrm{d}x - \frac{cC^2}{2},
\end{aligned}$$

and $\{v_n\}$ is bounded in $W^{1,1}(0,1)$. The Sobolev imbedding theorem asserts that $\{v_n\}$ is relatively compact in $L^1(0,1)$.

Now consider $w_n = \phi^{-1}(v_n)$. The formulas (A.1) and (A.5) imply that ϕ^{-1} is continuous, increasing and that

$$\big|\phi^{-1}(t)\big| \leqslant C + C|t|^{2/(k+2)}, \qquad \big|\phi^{-1}(t)\big|^2 \leqslant C + C|t|. \tag{A.7}$$

To prove that $\{w_n\}$ is relatively compact we show that every subsequence of $\{w_n\}$ has a L^2-convergent further subsequence.

Let $\{w_{n_l}\}$ be a subsequence of $\{w_n\}$. Then there are a subsequence of $\{v_{n_l} = \phi(w_{n_l})\}$, denoted by $\{v_{n_{l_m}}\}$, and $v \in L^1(0,1)$ such that $v_{n_{l_m}} \to v$ in $L^1(0,1)$ and $v_{n_{l_m}} \to v$ a.e. Then $w_{n_{l_m}} \to \phi^{-1}(v)$ a.e. Applying Vitali's convergence theorem [15, p. 203] to $v_{n_{l_m}}$, we find that for every $\varepsilon > 0$ there is $\eta > 0$, such that

for every measurable set E, $|E| < \eta$ implies $\int_E |v_{n_{l_m}}|\,dx < \varepsilon$ for all n. Then (A.7) implies

$$\int_E |w_{n_{l_m}}|^2\,dx \leqslant \int_E \big(C + C|v_{n_{l_m}}|\big)dx < C\eta + C\varepsilon.$$

Now Vitali's theorem applied to $\{w_{n_{l_m}}\}$ asserts that $w_{n_{l_m}} \to \phi^{-1}(v)$ in $L^2(0,1)$.

Let w be a cluster point of $\{w_n\}$, which means that there exists a subsequence $\{w_{n_l}\}$ such that $w_{n_l} \to w$ in $L^2(0,1)$ as $l \to \infty$. Fatou's lemma, the boundedness of $\epsilon_n^{-1} F_{\epsilon_n}(w_n)$ and (A.6) imply that

$$0 \leqslant \int_0^1 W(w)\,dx \leqslant \lim_{l\to\infty} \int_0^1 W(w_{n_l})\,dx = 0.$$

Now for a.e. $x \in (0,1)$, $w(x) = \alpha$ or β. If we consider $v_{n_l} = \phi(w_{n_l})$, then the boundedness of $\{v_{n_l}\}$ in $W^{1,1}(0,1)$, proved earlier, implies that $\phi(w)$, the L^1-limit of $\{v_{n_l}\}$, is a BV function [10, Theorem 1, p. 172]. Since $\phi(w)$ only takes two values, $\phi(\alpha)$ and $\phi(\beta)$, we obtain

$$\phi(w) = \phi(\alpha) + \frac{\phi(\beta) - \phi(\alpha)}{\beta - \alpha}(w - \alpha).$$

Hence, w is also a BV function. □

From Proposition A.2 and Lemma A.3 we deduce how the minimizers of $\epsilon^{-1}F_\epsilon$ and F_0 are related.

PROPOSITION A.4. *Let $\{\epsilon_n\}$ be a positive sequence converging to 0, and w_{ϵ_n} be a minimizer of F_{ϵ_n} in X. Then $\{w_{\epsilon_n}\}$ is relatively compact in X and each of its cluster points is a minimizer of F_0 in X.*

References

1. J. Ball and R. James, *The Mathematics of Microstructure*. Birkhäuser, to appear.
2. J. Ball, R. James, R. Pego and P. Swart, On the dynamics of fine structure. *J. Nonlinear Sci.* **1** (1991) 17–70.
3. P. Bates and A. Chmaj, An integrodifferential model for phase transitions: Stationary solutions in higher space dimensions. *J. Stat. Phys.* **95** (1999) 1119–1139.
4. P. Bates, P. Fife, X. Ren and X. Wang, Traveling waves in a convolution model for phase transitions. *Arch. Rational Mech. Anal.* **138** (1997) 105–136.
5. D. Brandon, T. Liu and R. Rogers, Phase transitions and hysteresis in nonlocal and order parameter models. *Meccanica* **30**(5) (1995) 541–565.
6. J. Carr, M. Gurtin and M. Slemrod, Structured phase transitions on a finite interval. *Arch. Rational Mech. Anal.* **86** (1984) 317–351.
7. A. Chmaj and X. Ren, Homoclinic solutions of an integral equation: Existence and stability. *J. Differential Equations* **155** (1999) 17–43.

8. G. Dal Maso, *An Introduction to* Γ*-convergence*. *Progress in Nonlinear Differential Equations and Applications*. Birkhäuser, Boston (1993).
9. J. Ericksen, Equilibrium of bars. *J. Elasticity* **5** (1975) 191–201.
10. L. Evans and R. Gariepy, *Measure Theory and Fine Properties of Functions*. CRC Press, Boca Raton, FL (1992).
11. R. FitzHugh, *Biological Engineering*, H. Schwan (ed.), McGrow-Hill, New York (1969).
12. R. Fosdick and D. Mason, Single phase energy minimizers for materials with nonlocal spatial dependence. *Quart. Appl. Math.* **54**(1) (1996) 161–195.
13. R. Fosdick and D. Mason, On a model of nonlocal continuum mechanics Part II: Structure, Asymptotics, and Computations. *J. Elasticity* **48** (1997) 51–100.
14. R. Fosdick and D. Mason, On a model of nonlocal continuum mechanics, Part I: Existence and regularity. *SIAM J. Appl. Math.* **58**(4) (1998) 1278–1306.
15. E. Hewitt and K. Stromberg, *Real and Abstract Analysis*. Springer, Berlin (1965).
16. S. Kartha, D. Krumhansl, J. Sethna and L. Wickman, Disorder driven pretransitional tweed in martensitic transformations. *Phys. Rev. B* **52** (1995) 803–822.
17. A. Khachaturian, *Theory of Structural Deformations in Solids*. Wiley, New York (1983).
18. M. Killough, A diffusion interface approach to the development of microstructure in martensite, PhD Thesis, New York University (1998).
19. R. Kohn and S. Müller, Surface energy and microstructure in coherent phase transitions. *Comm. Pure. Appl. Math.* **47** (1994) 405–435.
20. M. Luskin, On the computation of crystalline microstructure. *Acta Numerica* **5** (1996) 191–258.
21. L. Modica, The gradient of phase transitions and the minimal interface criterion. *Arch. Rational Mech. Anal.* **98** (1987) 357–383.
22. S. Müller, Singular perturbations as a selection criterion for periodic minimizing sequences. *Cal. Var. Partial Diff. Equations* **1** (1993) 169–204.
23. S. Müller, *Variational Models for Microstructure and Phase Transitions*, Lecture Notes. Max-Plank-Institut, Leipzig (1998).
24. R. Peierls, The size of a dislocation. *Proc. Phys. Soc.* **52** (1940) 34–37.
25. M. Pitteri and G. Zanzotto, *Continuum Models of Phase Transitions and Twinning in Crystals*. CRC/Chapman&Hall, London, to appear.
26. X. Ren and M. Winter, Young measures in a nonlocal phase transition problem. *Proc. Roy. Soc. Edinburgh A* **127** (1997) 615–637.
27. R. Rogers and L. Truskinovsky, Discretization and hysteresis. *Physica B* **233** (1997) 370–375.
28. A. Roytburd, Martensitic transformation as a typical phase trnsformation in solids. *Solid State Phys.* **34** (1978) 317–390.
29. M. Slemrod, Admissibility criteria for propagating phase boundaries in a Van Der Waals fluid. *Arch. Rational Mech. Anal.* **81** (1983) 301–315.
30. S. Timoshenko, On the correction for shear of the differential equation for transverse vibrations of prizmatic bars. *Philos. Mag. Ser. 6* **41** (1921) 744.
31. L. Truskinovsky, Equilibrium phase boundaries. *Soviet. Phys. Dokl.* **27** (1982) 551–553.
32. L. Truskinovsky, About the normal growth approximation in the dynamical theory of phase transitions. *Cont. Mech. Thermodyn.* **6** (1993) 185–208.
33. L. Truskinovsky and G. Zanzotto, Finite scale microstructures and metastability in one-dimensional elasticity. *Meccanica* **30** (1995) 577–589.
34. L. Truskinovsky and G. Zanzotto, Ericksen's bar revisited: Energy wiggles. *J. Mech. Phys. Solids* **44**(8) (1996) 1371–1408.
35. A. Vainchtein, T. Healey, P. Rosakis and L. Truskinovsky, The role of the spinodal in one-dimensional phase transitions microstructures. *Phys. D* **115** (1998) 29–48.